



# Radial growth decline in a tropical Andean treeline in Bolivia

Rose Oelkers<sup>1,2</sup>, Laia Andreu-Hayles<sup>1,3,4</sup>, Rosanne D'Arrigo<sup>1</sup>, Arturo Pacheco Solana<sup>1,5</sup>, Milagros Rodriguez-Caton<sup>1,6</sup>, M. Eugenia Ferrero<sup>6</sup>, Ernesto Tejedor<sup>7</sup>, Alfredo F. Fuentes<sup>8,9</sup>, Carla Maldonado<sup>8,9</sup>, Daniel Ruiz-Carrascal<sup>10</sup>

## Affiliations

1. Lamont-Doherty Earth Observatory of Columbia University, Palisades, NY 10964, USA
2. Department of Earth Science and Environmental Change, University of Illinois Urbana-Champaign, Urbana, IL, USA
3. Ecological and Forestry Applications Research Center (CREAF), Bellaterra, Spain
4. Catalan Institution for Research and Advanced Studies (ICREA), Barcelona, Spain
5. Department of Land, Environment, Agriculture and Forestry (TeSAF), University of Padua, 35020 Legnaro, Italy
6. Instituto Argentino de Nivología, Glaciología y Cs. Ambientales (IANIGLA), CONICET Mendoza, Argentina
7. Department of Geology, National Museum of Natural Sciences-Spanish National Research Council (MNCN-CSIC), Madrid. Spain
8. Herbario Nacional de Bolivia, Instituto de Ecología, Carrera de Biología, Facultad de Ciencias Puras y Naturales, Universidad Mayor de San Andrés, La Paz, Bolivia
9. Latin America Department, Science & Conservation Division, Missouri Botanical Garden, St. Louis, MO, USA
10. Innovation and Technological Development Directorate, Universidad EAFIT, Medellín, Colombia.

Correspondence to: Rose Oelkers [roelkers@ldeo.columbia.edu](mailto:roelkers@ldeo.columbia.edu)

**Abstract.** Relative to research efforts in higher latitudes, the impact of climate shifts in the tropical treeline remains understudied. Little is known about the tree growth dynamics and climate response at this treeline over the past few centuries, and at present under a rapidly changing environment. Here we provide information on recent changes in tree-ring patterns of *Polylepis pepeii* BB.Simpson, a tropical tree species that grows in a monospecific forest at the elevational treeline in the Andes-Amazon ecotone of Bolivia and identify factors that limit its radial growth. We first developed a ring width (RW) chronology spanning 1867-2018 C.E. using dendrochronological methods and independently verified annual periodicity with radiocarbon dating. The RW chronology indicates a significant ( $p < 0.01$ ) radial growth decline in *P. pepeii* since 1997, a trend that mirrors a decrease reported in other *Polylepis* species from the drier central Andes of South America. *P. pepeii* tree-ring width (RW) was mostly limited by mean, minimum, and maximum temperature and precipitation-during austral summer (November-January). Over the instrumental period (1981-2019) prior-year temperatures negatively affected current-year tree growth ( $p < 0.05$ ), while prior-year wet conditions were associated with higher growth ( $p < 0.05$ ). Gridded temperature records (1901-2019) showed a significant increase in minimum temperatures and a decline in the diurnal temperature range since 1967, which may reduce orographic convection and water availability at higher elevations where our forest is located. In situ daily measurements from dataloggers in the forest recorded higher temperatures and lower relative humidity values when data was available. Our results suggest less moisture availability associated with warming conditions was related to the observed tree-growth decline. If temperature continues to rise at current rates, one of the highest-elevation tree species on the globe, *P. pepeii*, could face severe consequences. This work provides insights into the past and historical trends of a tropical Andean treeline, which shows a recent decline also observed in other high-elevation forests (4657-4800 m.a.s.l.) of tropical South America ( $> 17^\circ\text{S}$ ).



## 36 **1 Introduction**

37 Temperature-limited treelines have been well studied in dendrochronology. In the Northern Hemisphere (NH), shifts in  
38 latitudinal and elevational treeline have been associated with the effects of global warming (Flynn et al., 2025). For instance,  
39 shifts in tree-ring width (RW) have been linked to upward recruitment and ecotonal shifts in forests in the Pyrenees (Batllori  
40 and Gutiérrez, 2008). In the European Alps (Paulsen et al., 2000) treeline advances may be associated with radial growth  
41 response to minimum temperature thresholds and interannual climate variations overall. A tree-ring network of dominant  
42 conifer species from the French Alps found a common radial growth signal since 1930, which may be attributed to a mix of  
43 land-use changes, minimum temperature increases and nitrogen deposition (Rolland et al., 1998). At latitudinal treeline in the  
44 Ural mountains, forest expansion and species densification was linked to summertime (May-June) warming (Devi et al., 2020).  
45 Overall, several studies across Eurasia found increases in growth in agreement with warming, although models predict that  
46 this positive relationship between growth and temperature will diverge in the future (Camarero et al., 2020). Conversely, some  
47 treeline sites in boreal North America have exhibited a negative growth response and decoupling of RW to recent warming  
48 trends, likely due to temperature-induced drought stress (e.g. (D'Arrigo et al., 2008, 2004; Jacoby and D'Arrigo, 1995;  
49 Wilmking et al., 2005) and references therein).

50  
51 By comparison to the northern latitudes, there has been little work at treeline and high mountain locations in South America,  
52 where tree-ring studies, in general, have been notably scarce (Andreu-Hayles et al., 2023; Groenendijk et al., 2025; Quesada-  
53 Román et al., 2022). The stability of tropical treelines and high-mountain communities under global warming has become of  
54 great concern in recent decades (Cuesta et al., 2020; Feeley et al., 2012, 2011; Macek et al., 2009; Young and León, 2006). A  
55 recent report for the IPCC (Hock et al., 2019) stated with high confidence that runoff from tropical glacier-melt has already  
56 reached its peak in some regions of the Andes and has led to decreases in agricultural yield in high mountain areas due to  
57 decreasing water availability (medium confidence). As for vegetation structure, climate change is projected to affect the extent  
58 and composition of Andean biomes, with greater effects at high-elevation areas in the tropical regions due to a consistent  
59 increase in temperature, while precipitation is projected to be highly variable with clear differences between eastern and  
60 western slopes along the Andes (Tovar et al., 2022).

61  
62 In South America, forests found near the mountain peaks in the Andes Mountains are often referred to as 'treeline' or high  
63 mountain areas in literature (Hock et al., 2019; Körner, 2012; Young and León, 2006) and the term used herein is used to  
64 describe the upper range limits of the tree species found in the region. Plot studies in the Peruvian Andes-Amazon found that  
65 the position of Andean timberline is limited by seed dispersal (Rehm and Feeley, 2013). Tree-ring studies have been critical  
66 to understanding the climate response of high elevation forests in South America. A study from the Peruvian puna (upper  
67 Andes) presented the first tree-ring chronology of *Escallonia myrtilloides* L.phil. (Requena-Rojas et al., 2021), a species often  
68 found at treeline in the tropical Andes (Zapata, 2013), in which the authors showed radial growth is positively related to



69 precipitation, and negatively correlated to temperature variability in this region. Also in the central Andes of Peru, *Requena-*  
70 *Rojas et al. (2020)* analyzed the tree rings from three *Polylepis* species, a genus that dominates the treeline forests of South  
71 America, and found these trees are slow-growing and sensitive to both current-year temperature and prior year precipitation  
72 changes. In subtropical regions, *Morales et al. (2004)* reported that changes in precipitation may be limiting growth in *Polylepis*  
73 *tarapacana* Phil. treelines in Argentina. On the other hand, in tropical montane forests in northern Argentina, the growth of  
74 different species appears to be regulated by temperature at the upper elevations of an altitudinal gradient (Ferrero et al., 2013).  
75 In the temperate *Nothofagus pumilio* (Poepp. & Endl.) Cuatrec. Andean treeline, temperature variability facilitates tree  
76 recruitment in northern and southern Patagonia, while the rate of seedling establishment can be strongly modulated by the  
77 interaction between temperature and precipitation driven by the Pacific Decadal Oscillation and the Southern Annular Mode,  
78 respectively (Srur et al., 2018, 2016). Yet, there was a radial growth decline in *Nothofagus pumilio* at a Chilean treeline site,  
79 where precipitation had increased (Álvarez et al., 2015), possibly suggesting a non-linear growth response of these forests to  
80 climate.

81

82 Here we describe a tropical treeline site for the species *Polylepis pepeii* BB.Simpson (Simpson, 1979), growing high elevations  
83 (3700 m.a.s.l.-4000 m.a.s.l.) in the Andes-Amazon corridor of Bolivia in South America. This site is located at upper forested  
84 limit of Bolivia's Madidi National Park (MNP), a hotspot for biodiversity within the vast Amazon forest, located just east of  
85 the Cordillera Real in tropical Andes. The hydroclimate of the Amazon-Andes ecotone in the MNP and broader region is  
86 primarily influenced by the South American Summer Monsoon (SASM), which peaks in the tropics during austral summer  
87 (December-February). Interannual to decadal sea surface temperature (SST) conditions in the Pacific and Atlantic Oceans  
88 (Paegle and Mo, 2002; Vuille et al., 2000) also impact climate in the region. Originating in the tropical Pacific, the El Niño  
89 Southern Oscillation (ENSO) system is the dominant mode of annual to decadal hydroclimate variability in South America  
90 and indeed the globe (e.g. Garreaud, 2009; Vera et al., 2006; Vuille et al., 2000). ENSO varies between warmer (El Niño) and  
91 cooler (La Niña) phases (Ropelewski and Halpert, 1987), and both extremes substantially impact precipitation and temperature  
92 conditions over tropical South America. The Atlantic sector also plays a major role in South American climate, as defined, for  
93 example, by tropical North Atlantic (TNA) and tropical South Atlantic (TSA) indices, which supply zonal moisture transport  
94 across tropical South America (Enfield et al., 1999; Good et al., 2008).

95

96 Complex topography in the Andean foothills contributes to a variety of microclimatic conditions and variable controls on tree  
97 growth, complicating efforts to directly compare large-scale patterns of climate and tree-ring variability (typically RW) within  
98 or between species in a stand. This complexity, and the forest dynamics of the humid Amazon Basin drive gradients in  
99 temperature and humidity, shaping patterns of vegetation (Fuentes, 2005), e.g. between the lower, drier forests near the Tuichi  
100 River (~850 m.a.s.l.) and the upper Andean treeline (~4400 m.a.s.l.). At present, only two tree-ring studies have been published  
101 for the MNP: one for *Juglans boliviana* (C.DC.) Dode (14°40' S, 68°41' W; 1300 m.a.s.l.) in *Oelkers et al. (2023)* and another  
102 by *Andreu-Hayles et al. (2015)*, the latter confirming the formation of annual rings in a *Pseudomedia rigida* (Klotzsch &



103 H.Karst.) Cuatrec. cross-section (14°33'S, 68°49'W; 1000 m.a.s.l). There is thus much need for additional dendrochronological  
104 research in this area, particularly at treeline and the greater forested ecotone between the Andes and Amazon Basin.

105  
106 In the MNP, mid-elevation woody species typically endure greater annual temperature and elevational ranges than lowland or  
107 highland species, based on monitoring studies (Montaño-Centellas et al., 2024). Species composition in the tropical Andes is  
108 often related to latitude and elevation as well (Malizia et al., 2020). Despite temperature-driven increases in tree mortality and  
109 species migration between 500-3600 m.a.s.l., above-ground biomass increased between 2003-2014 in eastern Andean forests  
110 (Duque et al., 2021). This increase was largely driven by intact old-growth forests, for which 30% of the regrowth was  
111 attributed to large-sized trees after disturbances. These studies provide information about spatial features of species distribution  
112 and abundance and carbon storage in the Andes-Amazon and specifically the MNP. The results herein add an additional,  
113 complementary dataset on annual radial growth patterns and climate sensitivity of an Andean treeline site not previously  
114 available.

115  
116 The geographic range of *Polylepis pepeii* (family Rosaceae; common name “Kenua” or “Queñoa”) spans from central Bolivia  
117 to northern Peru (Simpson, 1979) between 3550-4800 m a.s.l. (Espinoza and Kessler, 2022). The genus name *Polylepis* is  
118 derived from the Greek words ‘many layers’, describing multiple layers of compressed thin-bark sheets, a functional trait that  
119 allows these trees to adapt to cold temperatures at high elevation. The wide dispersion of leaves along the branches in *P. pepeii*  
120 and its long fruit distinguish this species from other *Polylepis* types. *P. pepeii* can reach significant age (>135 years) and the  
121 RW can be sensitive to prior and current-year climate (Jomelli et al., 2012; Roig et al., 2001).

122  
123 The *Polylepis pepeii* site investigated for this study is found between 3700~4400 m.a.s.l. in the western MNP (14°40'-14°43'S;  
124 69°04'-69°06'W). Located near the small settlement of Keara, vegetation is characterized as Alto-Andino Yungueño (Upper  
125 Andean Yungas) forest (Navarro et al., 2010) with a seasonally humid climate. This study area was chosen in part because  
126 inventory plots already exist at this location, established by botanists from the National Herbarium in La Paz (Bolivia) and the  
127 Missouri Botanical Garden (USA). In the following sections we: i.) generate a new RW chronology for *P. pepeii*, ii.) identify  
128 those climate variables (e.g. mean temperature or precipitation) that are the most limiting for annual growth and related trends  
129 and iii.) assess the impacts of extreme climate events on the RW variations. In so doing we demonstrate, through  
130 dendrochronological methods, the potential for this species to improve our understanding of growth trends and climate  
131 response of a tropical treeline in South America for dendrochronological studies.



132 **2 Materials and methods**

133 **2.1 Climate data**

134 Climatic Research Unit (CRU) station-based monthly temperature data V4.07 (Harris et al., 2020) and ground and satellite-  
135 derived rainfall data from the Climate Hazards Infrared Precipitation with Station group V2.0 (CHIRPS, accessed 2023; Funk  
136 et al., 2015) were used to extract monthly climatology and computing monthly and seasonal correlations with RW. The  
137 CHIRPS v2.0 (0.05°) dataset was used due to its higher spatial resolution relative to the CRU precipitation (0.5°) dataset.  
138 CHIRPS does, however, cover a shorter period (1981-2025) than the CRU record (1901- 2023). Monthly and seasonal climate  
139 data were based on the nearest gridpoint to each of the sites: for CRU average, minimum, and maximum temperature (0.5°)  
140 the gridpoint 14.75°S, 69.5°W and for the CHIRPS precipitation gridpoints (0.05°) we used 14.725°S, 69.12501°W.

141 **2.2 Site description and climatology**

142 Fig. 1 shows the location of the study sites in Keara and the landscape and vegetation patches of the high elevation *P. pepeii*.  
143 Climatology plots for the period 1981-2019 show that the wet season spans from ~October-April, with dry conditions (mean  
144 of 36-55 mm per month) from ~June-August (Fig. 1B). The monthly temperature data, limited by the spatial resolution of the  
145 CRU 4.07 gridpoint (0.5°×0.5°), shows mean temperature ranged from -8.2 to 14.5°C for the 1981-2019 period while mean  
146 annual precipitation (CHIRPS) was 1233 mm per year in Keara. Based on field sampling observations, the foliage of *P. pepeii*  
147 may be considered evergreen.

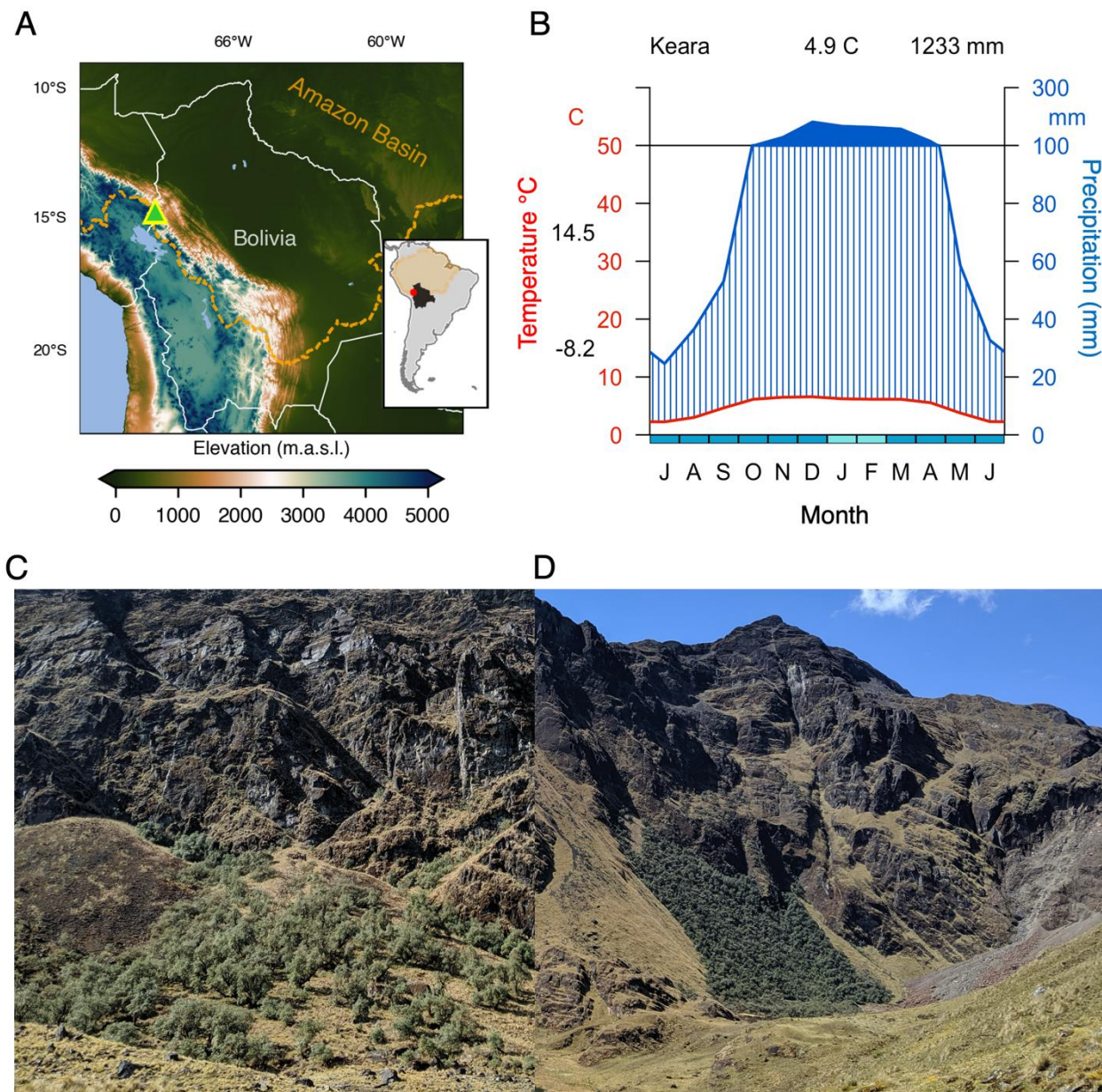
148  
149 Core samples of *P. pepeii* were extracted in October 2012 and July 2019. The 2012 collection was from an open-canopy south-  
150 facing forest west of the small community in Keara (3795~4000 m.a.s.l.; Fig. 1C), which was originally surveyed during an  
151 exploratory expedition. The 2019 collection was made southeast of Keara in a remote, closed-canopy west-facing stand in a  
152 high-elevation valley called Waca-cocha (after a lagoon near the sampling site) (4000-4400 m.a.s.l.; Fig. 1D). Both sites feature  
153 seasonally humid, upper-montane forests, with persistent mist that evaporates during the day. These sites are largely  
154 monospecific, dominated by fragmented patches of *P. pepeii* and small amounts of *Gynoxys compressissima* Cuatrec. trees. As  
155 noted, the bark of *P. pepeii* consists of thick layers of compressed flakes that are red and brown in color, characteristic of the  
156 genus (Fig. 2A). The trees are shrublike, with twisted (and at times, multiple) stems.

157  
158 Core samples were extracted from living trees using 2-threaded increment borers (5 mm in diameter). Cross sections of dead  
159 trees were sliced using a gas-powered chainsaw or standard saw-tooth blade. Stem diameter was measured at the same level  
160 that core samples were extracted (at breast height ~1.2 m). HOBO® temperature and relative humidity data loggers  
161 (<https://www.onsetcomp.com/>) were installed near the *P. pepeii* trees at 14°40'S 69°06'W (4158 m.a.s.l.) during the 2012 visit  
162 to Keara and data was recorded hourly from 1 September 2011 to 2 September 2014. New HOBO sensors were installed in  
163 the 2021 and collected during fieldwork in 2023. Unfortunately, the system batteries failed within 9 months of the launch, and



164 data was limited to only 20 September 2021 to 23 May 2022. Daily minimum, maximum and mean temperature and relative  
165 humidity were calculated from 20 September to 23 May (245 days) for the 2011-2012, 2012- 2013, 2013-2014 and 2021-2022  
166 periods. Kernel density estimates were used to generate and compare probability distributions among the daily time series and  
167 nonparametric Kolmogorov-Smirnov (KS) tests (Kolmogorov, 1933; Smirnov, 1948) were conducted to determine the  
168 significance of the difference between the timeseries. Kernel density and KS tests were conducted using seaborn (Waskom,  
169 2021) and SciPy (Virtanen et al., 2020) packages in *python*.

170



171

172

173 **Figure 1: (A) Location of *Polylepis* site near Keara in the Eastern Cordillera of the Andes-Amazon ecotone. (B) Monthly climatology**

174 **(1981-2019) for Keara based on minimum and maximum temperature from CRU 4.07 and precipitation from CHIRPS gridpoint**

175 **data. Photos of open-canopy (KEPP; C) and closed canopy (SP; D) forest patches which were sampled at altitudinal treeline in**

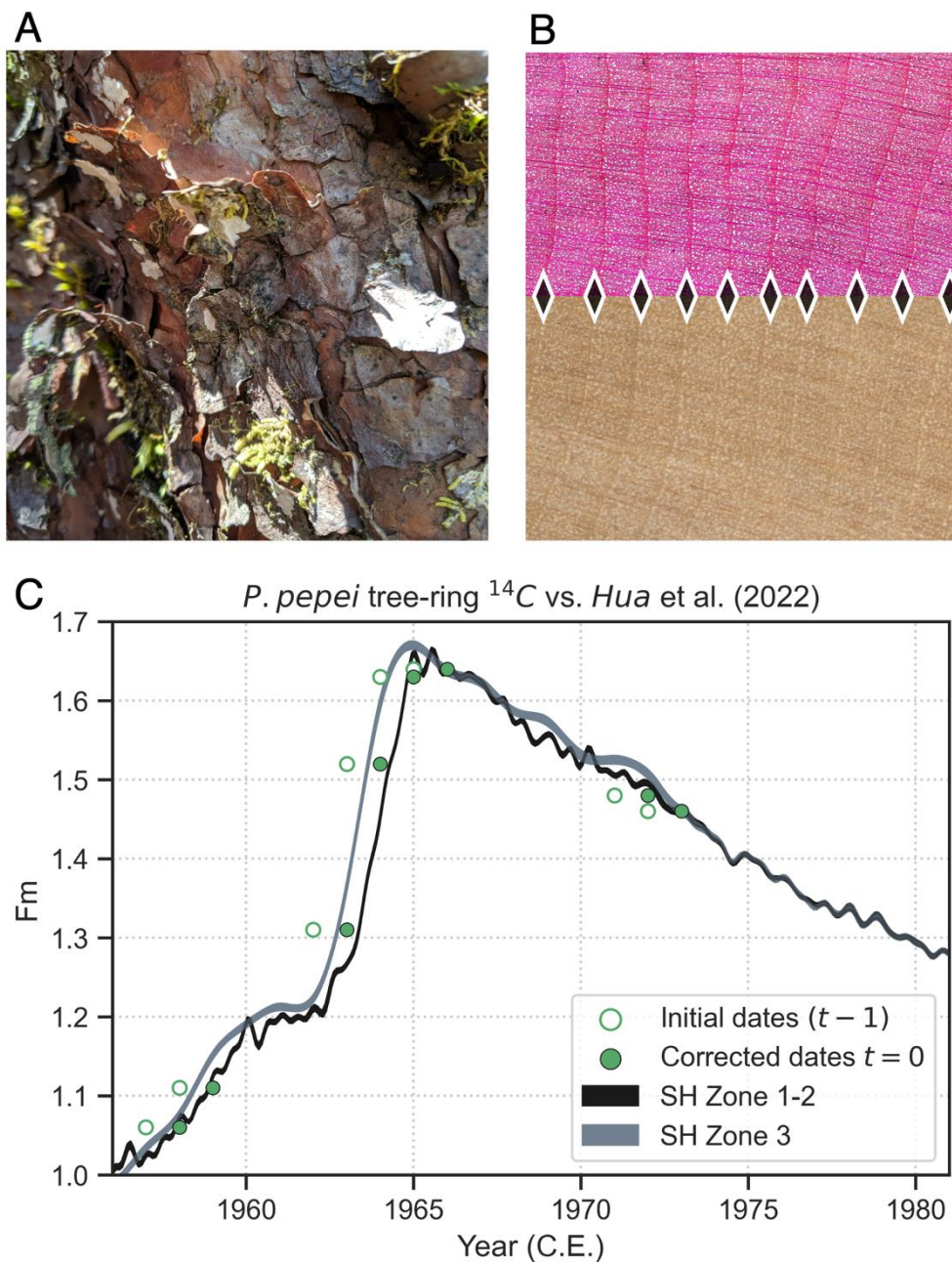
**Bolivia's MNP (~3700-4300 m.a.s.l.).**



176 **2.3 Wood processing and anatomical analyses**

177 Wood samples were shipped to the Lamont-Doherty Earth Observatory (LDEO) in NY, USA for dendrochronological analysis.  
178 Cores and cross sections were finely sanded up to 1000 grit using an orbital sander and manually polished with microfiber  
179 paper. Most samples had surficial color differences within the stem, mainly reflecting variable transitions between the  
180 heartwood (darker color, middle to interior of the stem) and sapwood (the active, lighter wood, beyond the cambium layer  
181 towards the outside of the stem). The lighter sapwood made ring characteristics difficult to visualize.

182  
183 To aid in identifying anatomical properties in the wood, histological (micro) cuts were performed according to techniques  
184 described in von Arx et al. (2016) using a WSL Core microtome (<https://www.wsl.ch/en/services-produkte/microtomes/>). *P.*  
185 *pepei* is an angiosperm with diffuse porous wood anatomy, which is typically harder to date than ‘ring porous’ wood, due to  
186 less distinct boundaries between the latewood of the prior year and the earlywood of the current year. *P. pepei* tree rings feature  
187 large, semicircular vessel elements in the earlywood that taper tangentially in size towards the transition to latewood, which  
188 has thicker, fiber-like tracheid cells (Fig. 2B; Roig et al. 2001).



189

190 Figure 2: Tree stem (A) and ring anatomy (B) of *P. pepei* samples. The direction of growth for the core and anatomical images is  
191 from left to right (pith to bark) while black diamonds indicate the latewood/earlywood boundary between annual rings. (C)  
192 Radiocarbon data measured in alpha cellulose from selected rings of the *P. pepei* tree-ring chronology (green circles) plotted with  
193 the Hua et al. (2022) reference curves SH Zone 1-2 and SH Zone 3.



## 194 2.4 Tree-ring chronology development

195 Tree rings were measured and dated visually using standard dendrochronological techniques (Stokes and Smiley, 1968). RW  
196 was measured digitally using the *CooRecorder* image analysis program (Cybis Elektronik, 2010). Before completion of the  
197 RW chronology, radiocarbon was conducted on a cross-section sample (SP20X; Figure 2C) collected in 2019 in the closed-  
198 canopy forest. This sample was chosen due to high correlation between the RW timeseries (1909-2018;  $r=0.51$ ) and 11 trees,  
199 named ‘KEPP’ from the 2012 expedition measured previously (1881-2012; overall correlation among samples:  $r=0.50$ ).  
200 Individual growth rings associated with the years 1957, 1958, 1962, 1963, 1964, 1965, 1971, and 1972 were sliced, extracted  
201 for cellulose, and processed for modern radiocarbon analyses to independently confirm annual resolution of the rings. All  
202 radiocarbon measurements were compared to the monthly SH  $\Delta^{14}\text{C}$  radiocarbon curve (1950-2019 C.E.) from the designated  
203 atmospheric Zones 1-2 and 3 (SH Zone 1-2; Hua et al., 2022).

204  
205 Initial radiocarbon results (Fig. 2C) showed that  $^{14}\text{C}$  measurements of SP20X were offset by 1 year in relation to the SH Zone  
206  $^{14}\text{C}$  curves. In the original *P. pepei* RW data generated with material collected in October 2012, the last ring (assigned as 2012)  
207 was not measured as it was considered an incomplete growth year. Upon a recent inspection of these samples, we observed  
208 that the final ring behind the bark did not always correspond to a partial ring as some trees had not yet started wood formation  
209 in 2012 (at least for the side of the stem where the core was sampled). Therefore, the calendar year assigned to the last complete  
210 ring for the KEPP RW samples were measured and corrected to 2011. This date-adjustment on the most recently formed ring  
211 behind the bark was confirmed after cross-dating RW from additional living trees collected in 2019 from the Waca-cocha  
212 forest. The updated KEPP RW chronology ( $n=13$  trees) showed high correlation with the newly developed SP RW chronology  
213 ( $n=15$ ; 2019 collection) indicating good agreement among all RW series for the Keara *P. pepei* network (combined mean  
214 correlation,  $r=0.46$ ).

215  
216 Once final calendar dates were assigned to the tree-ring samples, the Schulman convention (Schulman, 1956), which assigns  
217 each ring date to the year growth began, was applied. Individual RW time series from the 2012 and 2019 collection were  
218 detrended conservatively with age-dependent cubic splines (initial spline stiffness of 60 yrs) (Cook and Peters, 1981; Melvin,  
219 2004) and RBAR variance stabilization to account for changes in sample size through time (Frank et al., 2006). So-called  
220 “standardized” chronologies, which were compared to the climate data, were constructed by taking the ratio of the fitted and  
221 observed RW values of detrended time series and combined using a robust Tukey bi-weight mean to produce a dimensionless  
222 ‘standard’ RW chronology (Cook et al., 1990). The so-called “residual” RW is the prewhitened chronology for the Keara  
223 samples (i.e. autocorrelation is removed) determined by the Akaike information criterion with autoregressive modelling on the  
224 individual time series (Akaike, 1974). The residual chronology was used for i.) identification of small or large outliers in the  
225 chronology (top 5 and 95 percentiles) and ii.) for analyses of the growth response of *P. pepei* to extreme ENSO events (see  
226 section 2.6).



227 The subsample signal strength (SSS) was used to estimate the minimum sample size required to maintain a common signal  
228 (Wigley et al., 1984). SSS considers the declining population-size through time and is often used for climate reconstruction  
229 purposes (see discussions *Buras et al., (2017)* and *Wigley et al. (1984)*). The Pettit's (1979) changepoint detection test was  
230 used on the raw and standard RW to detect the timing and significance ( $p < 0.05$ ) of recent trends in growth. Significance of  
231 the growth shifts was determined using a Mann-Kendall test. Changepoint analysis was conducted using the 'trend' package  
232 in *R* (Pohlert, 2016).

### 233 **2.5 Temperature and precipitation signal in *P. pepei* growth rings**

234 To determine the relationships between the RW timeseries, temperature, and precipitation, monthly and seasonal Pearson  
235 correlations ( $r$ ) were computed via bootstrapped correlations using the 'treeclim' package in *R* (Zang and Biondi, 2015). Due  
236 to the covariance between temperature and precipitation in this region, we used the 'seascorr' function (Meko et al., 2011) to  
237 evaluate the significance of the correlation of temperature without the covariance with precipitation, and the other way around.  
238 Following methods of *Meko et al. (2011)*, partial correlation coefficients with temperature are obtained by: i.) first performing  
239 a linear regression between RW and precipitation ii.) calculating bootstrapped, partial correlations between temperature and  
240 the residuals from this regression, which represent the portion of RW variability not explained by precipitation. Thus, partial  
241 correlations show the relationship between tree-growth and temperatures without the influence of precipitation. Spatial  
242 correlations (significance  $p < 0.05$ ) were also computed to assess the extent of the temperature and precipitation signals of the  
243 RW records across space for the most significant season for each tree species.

244

### 245 **2.6 Superposed Epoch Analysis**

246 To investigate the effects of extreme climate events, including the potential impact of ENSO on tree growth, Superposed Epoch  
247 Analysis (SEA) was performed on the residual RW timeseries (Fig. 3B using the method originally described by *Haurwitz and*  
248 *Brier (1981)* and modified by *Rao et al. (2019)*. SEA is widely used to statistically determine whether the effects of episodic  
249 events (e.g. ENSO events) on a response variable (in this case RW) are statistically significant or due to random noise. The  
250 *Rao* method uses 1000 random-sample double bootstrapping to quantify the RW response at the time of the event ( $t = 0$ ) and  
251 several years after (in this case 4 years). Table 1 lists the years of known precipitation anomalies in tropical South America  
252 connected to El Niño (warmer) or La Niña (cooler) conditions in the Pacific Ocean.

253

254 The twelve top-ranked El Niño and La Niña years listed by the National Oceanic and Atmospheric Administration's Physical  
255 Science Laboratory (NOAA-PSL: <https://psl.noaa.gov/enso/>) based on the extended multivariate ENSO index (MEI.ext)  
256 (1871-2005) and MEIv2.ext (1979-2024) were used. This bimonthly dataset is based on the dominant modes, or principal  
257 components, of the entire tropical Pacific ENSO domain (30°N-30°S, 100E°-70°W) rather than any one region (e.g. Niño 3.4)  
258 and integrates observations of sea level pressure (SLP), sea surface temperature (SST), meridional (north-south) wind, and  
259 outgoing longwave radiation (MEIv2.ext) (see *Wolter and Timlin, 2011*). The ranking of extreme ENSO years is mainly



260 defined by SST anomalies during DJF, coincidentally when ENSO is phase locked with the peak monsoon season (Rasmusson  
 261 and Carpenter, 1982).

El Niño		La Niña	
1983	1987	1974	2008
			264
1998	1942	1917	1943
			265
1973	1988	1956	1956
			266
1931	1941	1976	1904
			267
1992	1995	2011	1999
			268
1966	1915	1989	1911
			269
1919	2003	1910	1959
			270
1926	1903	1971	1972
			271
1958	1900	1951	1909
			272
1897	1906	2000	2012
			273
2010	2007	1974	1925
			274
1983	1978	1917	1939
			275
1998	1980	1918	1962
			276
			277
			278

279 **Table 1: Years of climate events selected for SEA. The two left columns show the 24 top ranked DJF El Niño or La Niña years based**  
 280 **on the PSL Multivariate Extended ENSO index (1895-2015) ([https://psl.noaa.gov/enso/past\\_events.html](https://psl.noaa.gov/enso/past_events.html)).**

### 281 3 Results

#### 282 3.1 Growth decline in a *P. pepei* tree-ring chronology

283 The *P. pepei* RW chronology from northern Bolivia (max elevation 4400 m.a.s.l.) spans from 1868-2018 is shown in Figure 3.  
 284 Wood anatomy confirmed the earlywood and latewood diffuse-porous features of the rings (Fig. 2B) and radiocarbon  
 285 measurements (Fig. 2C) in selected years before and after the radiocarbon bomb-peak confirmed that the growth periodicity is  
 286 annual.

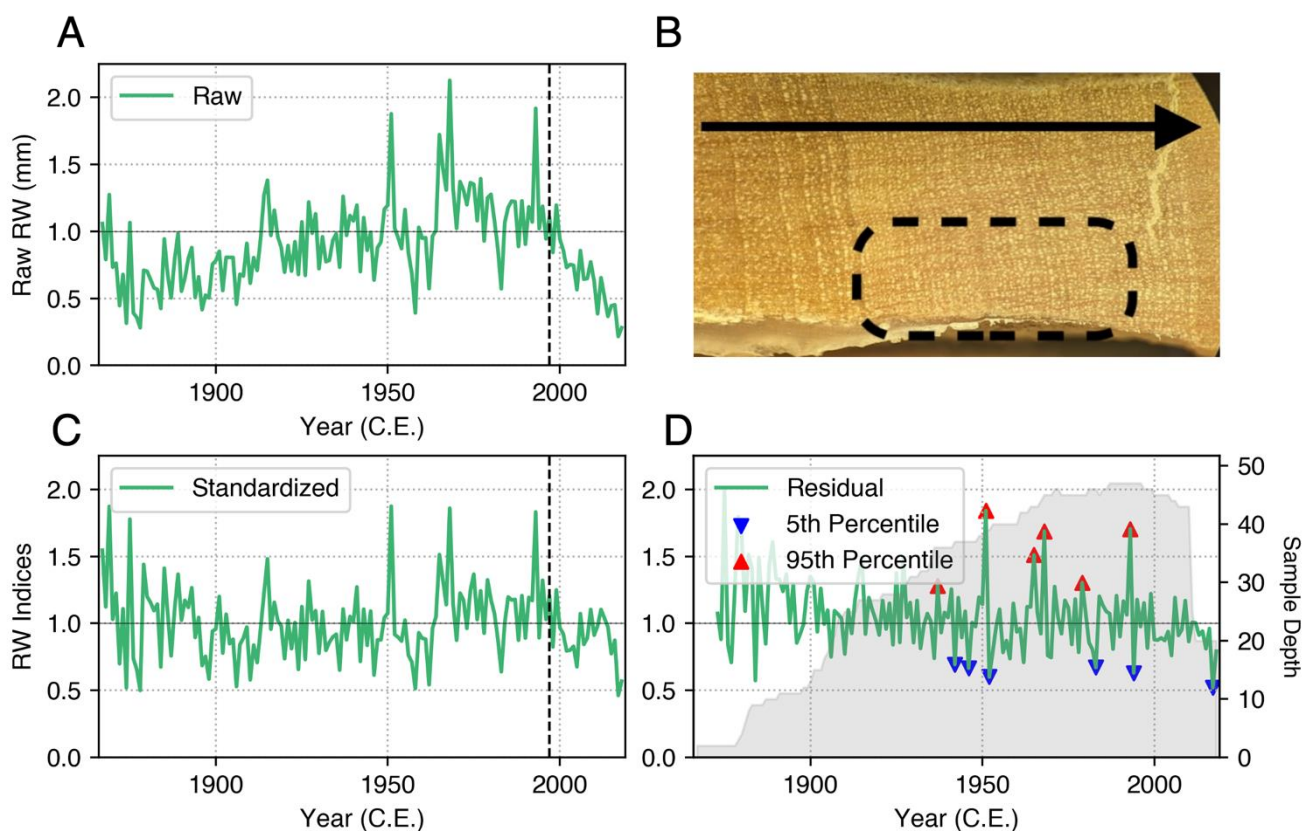
287  
 288 Due to extreme suppression in radial growth (Fig. 3B), only one or two cores per tree (out of 3-4 total) were able to be cross-  
 289 dated and used for the final RW chronology. Nevertheless, the individual trees shared a common coherency in the RW patterns



290 with a mean inter-series correlation of  $r = 0.46$  ( $n = 28$ ). The SSS metric indicated that *P. pepei* RW maintained a common  
 291 signal especially between 1909-2018 (average age of the samples 92 yrs) with 22 samples needed to reach such a threshold  
 292 (SSS > 0.85; Wigley et al. 1984). These trees were slow-growing with stem diameters (DBH) ranging from 10 cm to 54 cm  
 293 (mean DBH 33 cm) with an average radial growth of  $0.9 \text{ mm yr}^{-1}$ .

294  
 295 Notable growth years since 1909 are denoted as triangles in the residual RW timeseries (Fig. 3D). The plot indicates extremely  
 296 narrow or wide RW anomalies, mainly during the mid 20<sup>th</sup> century. Tree-ring values for 1957 and 1972 were in the 5<sup>th</sup>  
 297 percentile for *P. pepei*, indicating unfavorable environmental conditions for growth, while the year 1999 showed common  
 298 above-average growth. Raw RW has been declining steadily since the 1960s (Fig. 3A), especially after 1996 ( $p = 0.01$   
 299 determined by the Mann-Kendall and Sen's slope tests), with a less pronounced trend in the standard RW series (Fig. 3C).

300



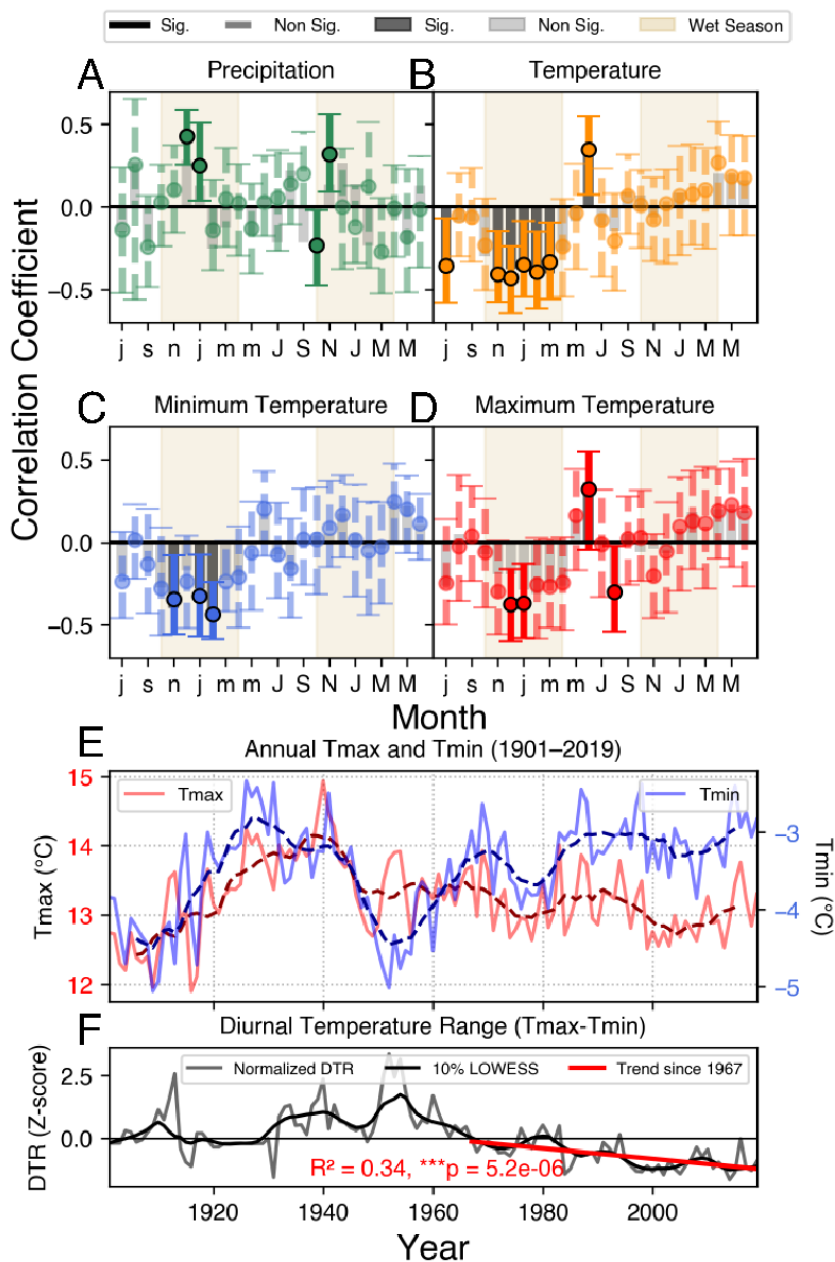
301  
 302 **Figure 3: Raw (A), Standard (B), and Residual (C) RW chronologies compiled using *P. pepei* trees from Keara. (A) The raw data**  
 303 **shows a decreasing RW trend since 1996/97 (black-dotted line). (B) An image depicts tight growth observed in a core sample where**  
 304 **several rings are suppressed within a 4 mm distance (dashed circle). The black arrow indicates the direction of growth for this image**  
 305 **(from left to right). The residual chronology is plotted with changing mean sample size (shaded color) for the site through time (D).**  
 306 **Triangles on the residual timeseries denote the years within the top 5<sup>th</sup> (smallest growth rings; Blue color) and 95<sup>th</sup> (largest growth**  
 307 **rings; red color) percentiles between 1909-2018.**



### 308 **3.1 Monthly climate-growth relationships**

309 Monthly correlation analysis for the period from July 1981 to June 2018 shows negative correlations with temperature and  
310 positive correlations with precipitation during growing seasons. *P. pepeii* RW shows significant positive correlations with  
311 December-January precipitation from the prior wet season (Fig. 4A), with established strong and consistent negative  
312 relationships with mean temperatures for an extended season from November to March during the prior wet season (Fig. 4B).  
313 Negative, significant correlations were found between *P. pepeii* RW and prior season November, January, and February  
314 minimum temperatures (Fig. 4C), as well as with December and January maximum temperatures (Fig. 4D). Partial correlations  
315 indicate the relationship between temperature and RW was more significant independent of precipitation variability (i.e. the  
316 negative mean and minimum temperature signal persists even when the covariance with precipitation is removed).

317  
318 A robust, negative, temperature relationship with tree growth between 1981-2019 occurs during a period when minimum  
319 temperatures have continuously increased since (Fig. 4E). Further, the diurnal temperature range (i.e. difference between  
320 maximum and minimum temperature) depicts a significant negative trend in this region since 1967 which means the rate of  
321 increase for minimum temperatures has surpassed that of maximum temperature (Fig. 4F). It is interesting to note an extreme  
322 cold period observed in annual temperature data the late 1950s (Fig 4E) also corresponds with a growth suppression observed  
323 in *P. pepeii* RW in Figure 3A and C.



324

325

326

327

328

329

330

331

332

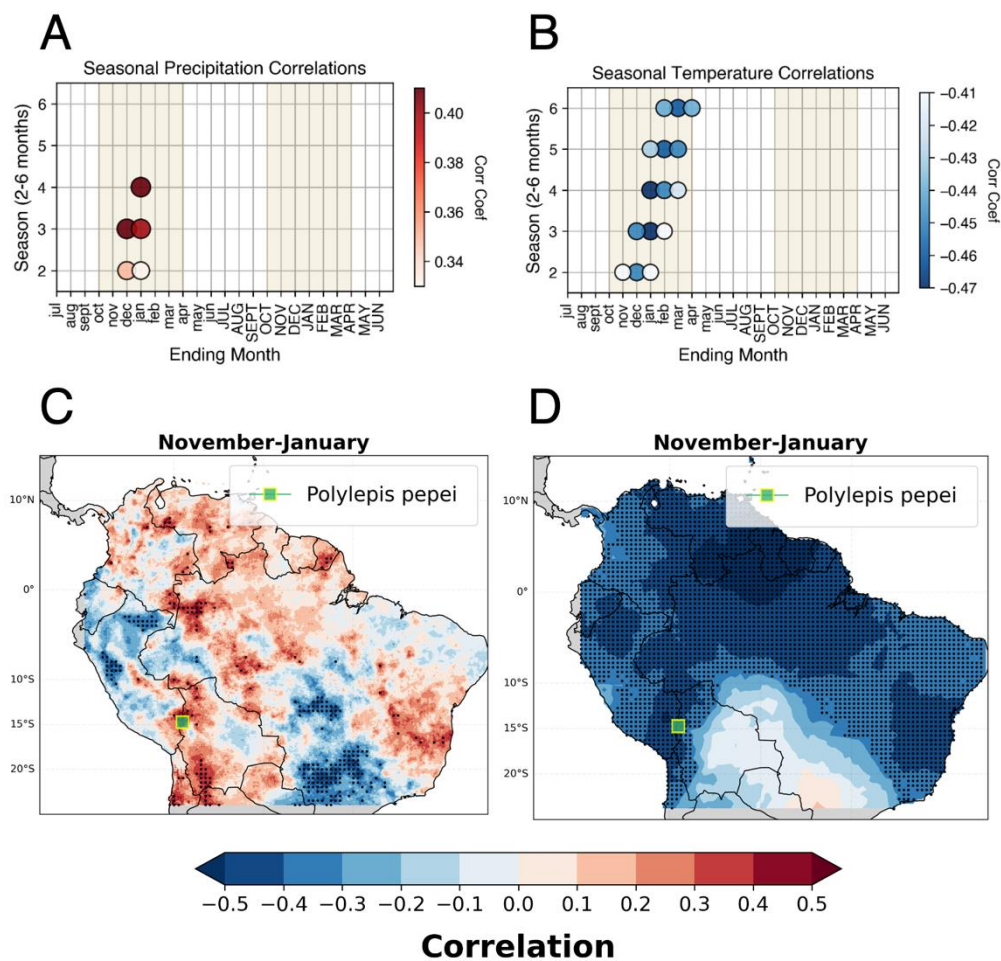
**Figure 4: Monthly RW-climate correlations (1981-2019).** Pearson correlations ( $p < 0.05$ ) between precipitation from CHIRPS (A) and mean, minimum, and maximum temperatures from CRU (B-D) for grid points closest to the sites. The x-axis represents months beginning in July of the prior-year ( $t-1$ , lowercase letters) and extending to June of the current year ( $t=0$ , uppercase letters). Tan shading indicates the extended wet period (October- April) for this region of the MNP. Significant correlations are represented by solid lines. Solid gray bars show partial correlations with a given variable. (E) Annual minimum (blue line) and maximum (red line) temperatures between 1901-2019 for the nearest CRU gridpoint. (F) The normalized diurnal temperature range, calculated as the difference between Tmax and Tmin, is plotted with a 10-yr smoothing spline and linear trend line since 1967. The  $R^2$ -value and significance of the 1967-2019 trend are included as red text.



### 333 **3.3 Seasonal and spatial climate sensitivity in *P. pepei* RW**

334 The prior-year climate signal in *P. pepei* RW at treeline is even more robust when compared to seasonal-averages of climate  
335 averaged for 2-months or more between 1981-2019 (Fig. 5). Correlations for 2-6 month averages reveal significant  
336 relationships ( $p < 0.05$ ) between RW and precipitation (Fig. 5A) or temperature (Fig. 5B). The standard RW chronology  
337 correlates the strongest with the 3 and 4-month averages of climate, particularly for prior-year OND and NDJ for both  
338 temperature and precipitation. Correlations include a positive relationship to precipitation with OND  $r = 0.41$  and NDJ  $r = 0.40$   
339 and temperature OND  $r = -0.45$ ; NDJ  $r = -0.47$  respectively. Because the highest correlation with climate included the negative  
340 NDJ relationship to temperature, this season was selected for illustrating regional correlations in Fig. 5C, D.

341  
342 Spatial correlations reveal the broader, regional extent of the climate signal recorded in the *P. pepei* RW record between 1981  
343 and 2019 (Fig. 5C, D). Regarding precipitation, *P. pepei* RW is positively correlated to seasonal precipitation in most of  
344 tropical South America (Fig. 5C). The strongest precipitation signal (indicated by black dots) is observed locally, extending to  
345 the eastern flanks of the central Andes in Bolivia and drier regions in the Southern Altiplano. Spatial patterns of correlation  
346 between *P. pepei* RW and gridded temperatures show significant and negative ( $r > -0.50$ ) correlations between 1981 and 2018  
347 across most of tropical South America during November to January (Fig. 5D). Note because the gridpoint data for the site  
348 confirmed temperature and precipitation are negatively correlated during the summer season (November-January;  $r = -0.40$ ,  $p$   
349  $< 0.05$ ), the negative correlations with temperature would reflect the indirect effect of temperature on water availability. The  
350 spatial variability of RW to precipitation account in figure 5D reflects heterogeneity of precipitation data in mountain areas,  
351 whereas the temperature fields are more uniform.



352

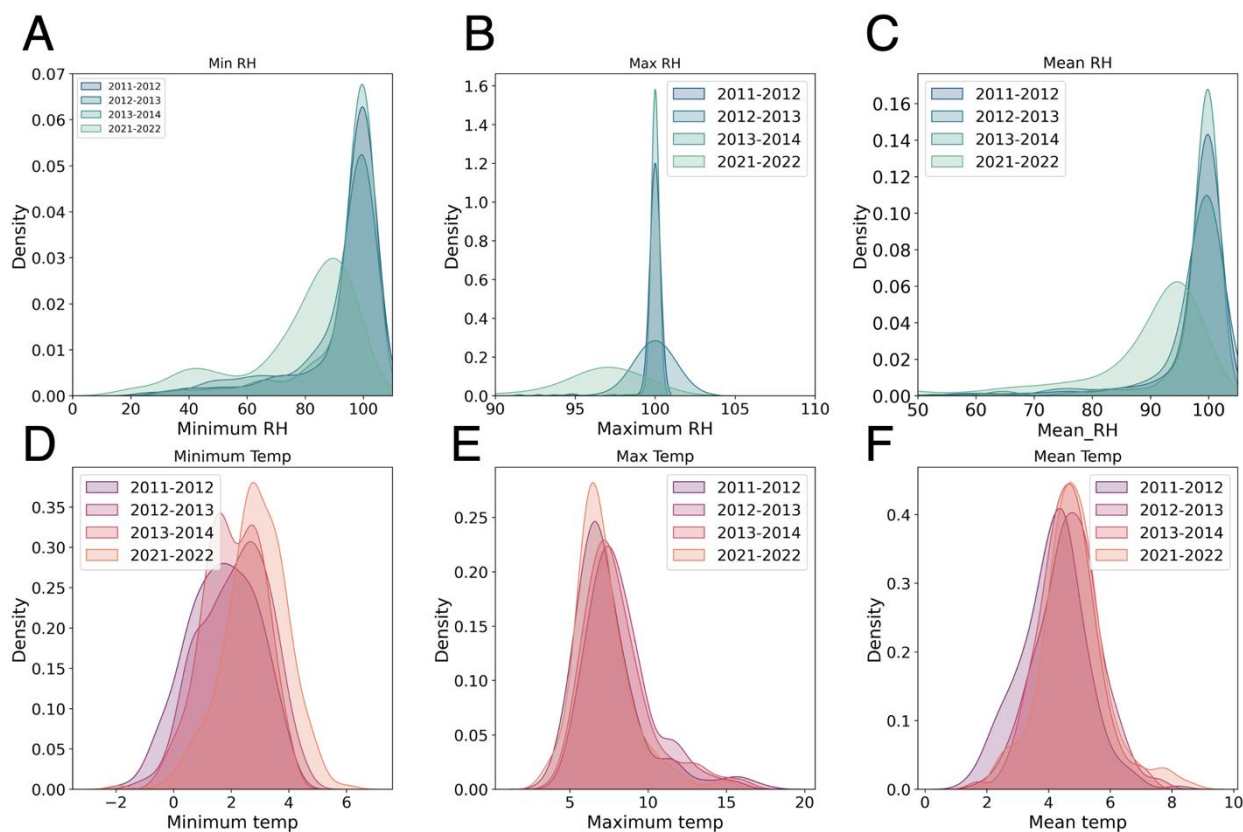
353 **Figure 5.** Precipitation (A) and temperature (B) seasonal correlations are shown. The color of the circles represents the value and  
 354 sign (+ or -) of Pearson correlations (see right-side color bars for r values' reference). The x-axis represents the months in which the  
 355 averaged seasons end (e.g. if the circle is in January, the season is November-January. The prior-year period of months is represented  
 356 as lowercase letters and the current period is represented as uppercase letters. The yellow shading represents the wetter period  
 357 between October-April based on the monthly climatology. Spatial correlations between RW- NDJ precipitation (C) and temperature  
 358 (D) for the period 1981-2019. Black dots represent the areas where there are significant correlations ( $p < 0.05$ ). RW is lagged  $t-1$   
 359 to account for the seasonality of the prior-year growing season. The NDJ season was selected based on moving bootstrapped seasonal  
 360 correlations with gridpoint data in (A,B).

### 361 3.4 Daily temperature and relative humidity recorded near the *P. pepeii* treeline

362 Probability density functions showed changes in the distribution of daily relative humidity and temperatures and among three  
 363 years between September 20-May 23. Minimum, maximum and mean relative humidity (RH) in 2021-22 was significantly  
 364 lower ( $p < 0.0001$ ) than in 2011-12, 2012-13, and 2013-14. A significant increase in minimum temperature range was reported  
 365 between the 2021-22 wet season as well as the three other wet seasons ( $p < 0.0001$ ), while non- significant differences were  
 366 observed between the 2021-2022 dataset and maximum temperatures in 2011-12 ( $p = 0.78$ ), and the mean temperatures in



367 2012-13 ( $p= 0.33$ ) and 2013-14 ( $p= 0.16$ ). Interestingly, daily maximum temperature in the 2021-2022 year is significantly  
 368 lower than the 2012-13 and 2013-14 seasons ( $p< 0.0001$ ). Although 2011-2012 was considered a major La Nina year (Table  
 369 1), the distribution of daily relative humidity values of 2012-13, 2013-14 are similar to the 2011-12 period, and all three seasons  
 370 had higher values than of (min, max, mean) RH than in 2021-22. Conversely, the range of minimum and maximum  
 371 temperatures were higher overall than the other three years.



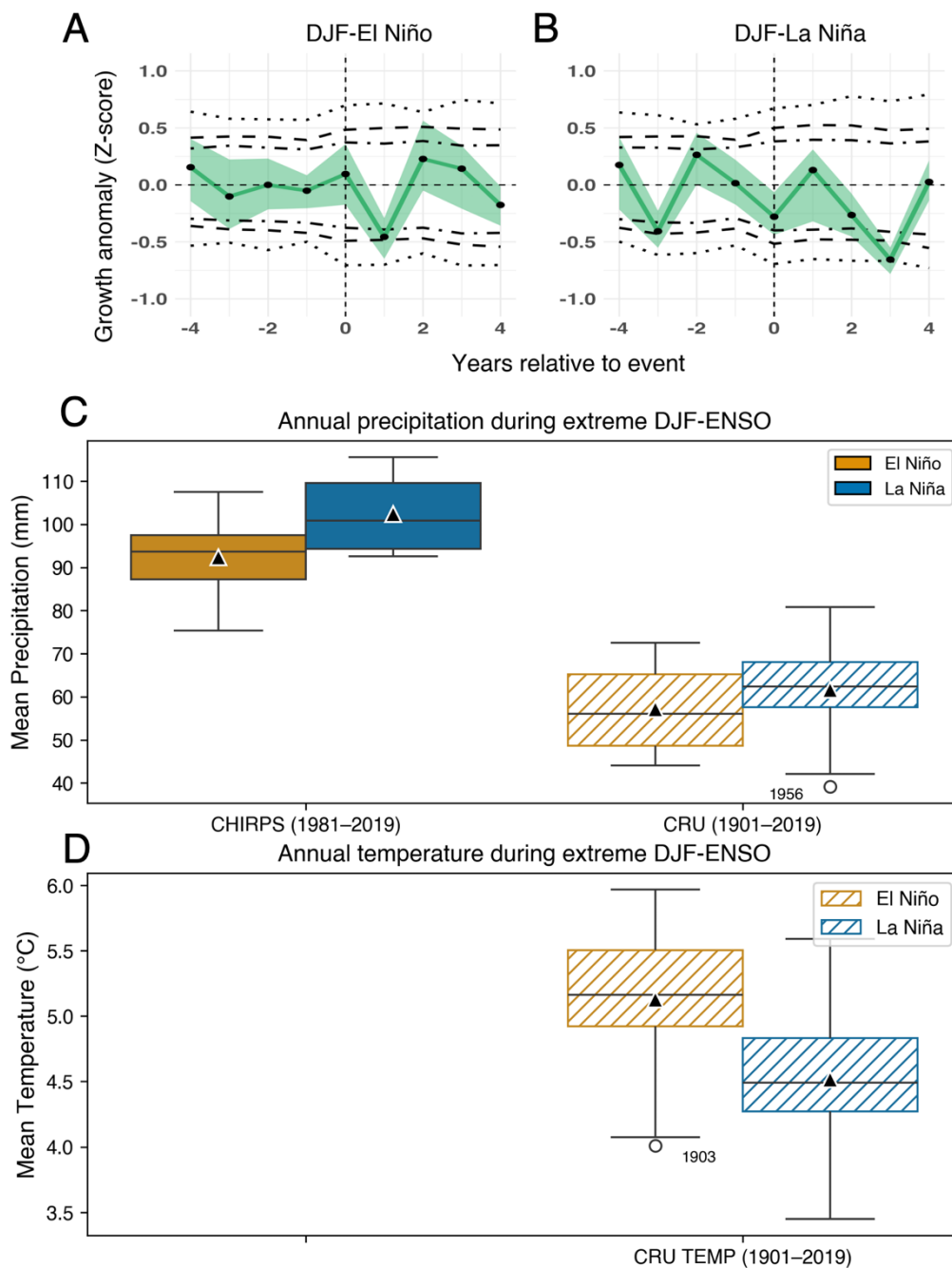
372  
 373 **Figure 6: Probably density plots of daily relative minimum, maximum and mean relative humidity (RH) (A-C) and**  
 374 **temperature (D-F) recorded for the wet season (September-May) of the years 2011-2012, 2012-2013, 2013-2014 and**  
 375 **2021-2022.**

376 **3.5 Growth response of treeline *P. pepei* to extreme climate events**

377 The impact of extreme DJF-ENSO events (Table 1) on residual RW (Fig. 3B) were conducted using SEA methods (Fig. 7A,  
 378 B). Normalized growth anomalies (Z-scores) are shown for the four years before and after the event ( $t=0$ ) to assess the timing  
 379 and significance of the RW anomaly. The impact of drought during El Niño years shows a lagged ( $t+1$ ) and negative growth  
 380 response ( $p< 0.10$ ; Fig. 7A), which means that one year after the event, *P. pepei* decreased radial growth. There are also  
 381 significant 3-year lagged negative responses during the extreme DJF-La Niña years, respectively (Fig. 7B).



382 Figure 7C shows boxplots of mean annual precipitation from the CHIRPS (1981-2022; ~5 km resolution) and CRU (1901-  
383 2022; ~55 km resolution) products for the top 24 years of extreme DJF-ENSO events (Table 1), while Fig. 7D includes annual  
384 mean temperature from the CRU gridpoint. Regardless of the time span and spatial resolution, both precipitation datasets show  
385 that the 24 El Niño extremes during the peak wet-season (DJF) are linked to drier conditions in the study region, and DJF-La  
386 Niña events were associated with wetter annual precipitation overall. CRU temperature data showed El Niño conditions were  
387 also warmer (Figure 7D). Overall, warmer and drier DJF ENSO events were associated with a smaller growth ring in the  
388 following year for *P. pepei*.



389

390

391

392

393

394

395

**Figure 7: Superposed epoch analysis of the residual RW response before ( $t-4$ ), during ( $t=0$ ), and after ( $t+4$ ) years of known to the top 12 DJF-El Niño (A) and DJF-La Niña events (B). Dashed black lines represent confidence intervals (two-tailed significance thresholds: 90%, 95%, 99%) based on double bootstrapping while the uncertainty of the response is depicted as green shading. (C) Annual precipitation boxplots using the CHIRPS (left) and CRU gridpoints for the (top 24) years of extreme DJF-ENSO, using the nearest. El Niño-related events are represented in orange colors, while La Niña is shown blue. (D) Annual temperature during these events using CRU gridpoint data.**



396 **4. Discussion**

397 **4.1. Radial growth decline and climate sensitivity of a tropical treeline site in Bolivia**

398 Annual RW chronologies of *P. pepei* from a high Andean, seasonally humid forest in northwestern Bolivia have been presented  
399 and analyzed. A new annually-dated tree-ring chronology for the MNP provides novel and robust information about tree  
400 growth at the tropical treeline (4000-4400 m.a.s.l.) in an understudied biodiversity hotspot in South America. There is a decline  
401 in mean radial growth that is particularly pronounced since 1997 (Fig 3C). This decline can also be seen visually in some  
402 samples from the drier (talus-slope) site in Keara (Fig 1C). The potential human influence on RW for trees in Andes-Amazon  
403 forests should be considered when evaluating the growth patterns of these Andean forests. For the *P. pepei* near Keara, the  
404 lower elevation open-canopy subset (~3700-4000 m.a.s.l.; north and west of the talus slope site) showed possible fire scars in  
405 the 1940s and clear forest fragmentation related to cattle ranching. This subpopulation is likely more threatened by human  
406 activities than the closed canopy site between 4000-4400 m.a.s.l. (Figure 1C). Nevertheless, dendrochronological approaches  
407 made it possible to explore the climate signal recorded in the annual rings.

408  
409 We found that *P. pepei* RW is limited by prior-year temperature variability and precipitation during the wet season, with larger  
410 RW in the subsequent growth year when it was wetter and colder. Although RW-precipitation correlations were robust, our  
411 results suggest that this *P. pepei* network is likely more affected by temperature-related moisture-stress changes, as would be  
412 expected particularly at elevational treeline (Fritts, 1976). Extreme El Niño and La Niña events during the peak summer  
413 monsoon bring dry/warm and wet/cool conditions may amplify or reduce the effect of precipitation and temperature variability  
414 on *P. pepei* growth. Overall DJF-El Niño events had a significant negative impact on radial growth of *P. pepei* at our study  
415 site. Although La Niña SEA were inconclusive, the lagged 3-year negative effect may be related to the occurrence of El Niño  
416 events in years after La Niña. DJF events were selected for analyses because it is the mature phase of the summer monsoon  
417 where the tropical Andes receives 70% of annual rainfall, but annual or NDJ related ENSO events may show larger impacts  
418 on trees studied herein.

419  
420 Future advances of this treeline (Fig 1C) are unlikely due to local geomorphologic constraints (Macias-Fauria and Johnson,  
421 2013) and thermal niches (Kessler et al., 2014; Körner and Hoch, 2023) that are requirements for subalpine recruitment. Studies  
422 of *P. pepei* sites between 3800~4300 m.a.s.l. in Peru (Kessler et al., 2014) and Bolivia (Hoch and Körner, 2005) recorded soil  
423 temperatures (> 5cm) ranging from 3-5°C during the wet season, highlighting the cold-adapted conditions of this species in  
424 the eastern tropical Andes. Despite local soil conditions and human activities that impact the shape of Andean treelines like  
425 those for *Polylepis* (Bader et al., 2007), the optimal thermal niche for woody plants is the leading abiotic factor that defines  
426 the spatial extent of such forests across the globe (Hertel and Wesche, 2008; Hoch and Körner, 2005; Körner and Hoch, 2023).  
427 In addition to the existing constraints for treeline advances, we report on the adverse influence of increased temperature on  
428 tree growth. We also report a growth decline that could be the result of these constraints. Although the future extent of the *P.*



429 *pepei* forest under is uncertain, our study provides insight into the limiting factors to radial growth at a tropical Andean treeline  
430 in Bolivia since 1981.

431

#### 432 **4.2. Changes in minimum temperatures and relative humidity at the *P. pepei* treeline in Bolivia**

433 Increases in minimum temperature may be reducing moisture availability in high-elevation Andean tropical sites. Although  
434 the shortness of the high-resolution CHIRPS dataset limits our interpretation of the role of climate before 1981 on observed  
435 growth trends, the long-term CRU temperature datasets show a significant decline in the diurnal temperature range (Fig. 4F),  
436 driven by rising minimum temperatures (Fig. 4 E).

437

438 In agreement, daily climate recorded in the data loggers in the *Polylepis* forests (Fig. 6) confirmed September-May in 2021-  
439 2022 as having significantly warmer nighttime/early morning conditions (reflected by minimum temperatures) in comparison  
440 to the period 2011-2012 ( $p < 0.0001$ ). Despite the fact that higher temperatures increase the capacity of the air to hold more  
441 water vapor (i.e. “Clausius-Clapeyron” relation), if the moisture supply does not increase proportionally the humidity will  
442 decrease. This is indeed what was observed from the RH data recorded *in situ* that showed significant decreases in minimum,  
443 maximum and mean RH at our study forests. In short, a decrease in RH alongside an increase in temperature suggests that the  
444 capacity of air to hold moisture has outpaced the actual moisture content, making the air drier despite higher temperatures.  
445 Further, analyses of gridded CRU temperature and local CHIRPS precipitation data near the *P. pepei* site are inversely  
446 correlated during the extended wet season (October-April). For example, if there is less cloud cover (and less precipitation)  
447 there is higher solar irradiance and temperatures, which may limit the photosynthetic capacity of these trees at higher elevations  
448 (García-Núñez et al., 2004; Hoch and Körner, 2005; Jaramillo, 2015). Although it is possible the timing of the mechanisms  
449 controlling primary (photosynthesis) and secondary growth (wood formation) may not occur at the same time, the RW-climate  
450 correlations show there is less radial growth if is warmer and drier than when it is cooler and wetter (Figs. 4 and 5).

451

452 Minimum temperatures influence convection, as rainfall in the Andes-Amazon ecotone largely occurs in the afternoon/night  
453 as radiative cooling drives cold air downslope and converges with rising warm moist air from the tropical lowlands (Garreaud,  
454 1999; Junquas et al., 2018; Romatschke and Houze, 2010). Known as ‘orographic precipitation’, this process is key for rainfall  
455 distribution across elevations in the Andean foothills like our study area (Arias et al., 2021; Chavez and Takahashi, 2017). A  
456 study on southern Peruvian rainfall hotspots (which included our study area in MNP) used radar-based precipitation data to  
457 analyses the relationship between rainfall and terrain elevation from 1998 to 2012. Maximum precipitation was found to peak  
458 annually between 1000-1300 m.a.s.l., with a vertical decrease in moisture distribution above 3000 m.a.s.l. (Chavez and  
459 Takahashi, 2017). However, if minimum temperatures are warmer, the radiative cooling effect is weaker, which means that  
460 warm, moist air may converge at lower elevations (Romatschke and Houze, 2010), below our treeline *P. pepei* site.

461



462 Therefore, the increase in annual minimum temperatures since the late 20<sup>th</sup> century in addition to an observed weakening of  
463 upper-level easterlies towards the Andes (Segura et al., 2022) may have contributed to reduced orographic convection, and  
464 thus moisture availability at high elevations, potentially limiting growth of *P. pepei*. Although our dataloggers covered a short-  
465 term window, the results provide *in situ* evidence of significant increases in minimum temperature and reductions in RH  
466 between the 2011-2014 and 2021-2022 seasons (September-May).

467

#### 468 **4.3. Growth declines related to changes in local environmental conditions**

469 Besides inhibiting moisture convergence and transport from lower elevations, warmer minimum temperatures could also affect  
470 the local soil-water balance by increasing transpiration, respiration rates and overall water loss in this forest (Sierra et al.,  
471 2022). From an ecophysiological perspective, respiration rates increase with rising temperatures. Without photosynthesis at  
472 night, this condition increases the amount of carbon (and water) released to the atmosphere and could negatively impact the  
473 life cycle and carbon sink capacity of the forest. A global analysis of tropical tree longevity using tree-ring and other data  
474 found that tree mortality is increasing in all tropical biomes due to heat-related water stress, with increased evaporative demand  
475 at the leaf level (Locosselli et al., 2020). The loss of smaller trees at the mid-high elevations has also been observed in a forest-  
476 biomass plot study across the Andes-Amazon (Duque et al. 2021).

477

478 It is important to note that the MNP and vicinity is not strictly undisturbed. In fact, illegal mining and logging activities have  
479 deteriorated forest structure and health, with increasing loss of forest cover in recent years (Finer and Mamani, 2023). Prior to  
480 the designation of Madidi as a National Park in 1995, large swaths of economically-valuable trees along riverbanks (e.g.  
481 *Amburana cearensis* Smith) were harvested for timber (Macía, 2008). Today, *P. pepei* studied herein, is at great risk of  
482 endangerment due to habitat loss related to fires and land conversion for cattle ranching (Espinoza and Kessler, 2022; Kessler  
483 et al., 2014). These losses of primary forests have severe implications for carbon storage capacity, ecosystem function, and  
484 land stability, all critical factors for the survival of native inhabitants. Herein, efforts were made to minimize potential impacts  
485 of land use and disturbance in field sampling, but ecosystem disturbances in certain regions of the MNP were nevertheless  
486 observed.

487

488 Overall, the negative correlations with temperature may reflect the indirect effect of temperature on water availability. High  
489 temperatures increase forest evapotranspiration as well as direct evaporation from the soil, thus reducing the amount of water  
490 available for growth. Furthermore, due to the observed increase in minimum temperature the high elevation *P. pepei* forest  
491 may be experiencing higher respiration rates at the same time receiving less moisture due to a reduction in orographic  
492 precipitation to higher-elevations. This may be resulting in the observed growth decline in most of the sampled trees. Although  
493 the changepoint tests detected increases in the long-term minimum temperature (e.g. 1967) that occurred earlier than the *P.*  
494 *pepei* RW significant decline (e.g. 1997), we may consider first that the statistics are just detecting a turning point in the data,  
495 and second that biological processes do not always occur at the same time as changes in environmental variables. In other



496 words, *P. pepei* response to changes in minimum temperatures and RH do not have to be linear and can be determined by  
497 thresholds. Nevertheless, the correlations with climate are robust and as described below, the timing of the decline may signify  
498 a response to regional shifts in hydroclimate patterns observed in the greater tropics of South America.

499

#### 500 **4.4. Large-scale climate variability impacting tree growth in tropical Andean treelines**

501 The recent decline observed at our *P. pepei* site in MNP (14°S) near the southwestern Amazon Basin aside from factors  
502 described above may be also influenced by broader scale hydroclimate changes. Negative growth at Andean treelines has been  
503 reported by *Morales et al. (2023)* of *P. tarapacana* tree rings from southern Peru and Chile (>17°S; 4657-4800 m.a.s.l.). The  
504 authors developed a NDJ precipitation reconstruction from these trees noting a drying trend since 1997 that is unprecedented  
505 within the time span from 1625 to 2013 CE covered by this 389-year chronology, and which was attributed to drought  
506 conditions that have increased in frequency and severity since the 1970s. Studies of *P. tarapacana* conducted in other areas of  
507 the Altiplano suggest that the species germination and distribution is projected to decrease as vapor pressure deficits,  
508 temperatures, and overall aridity increases (*Cuyckens et al., 2016, 2016; López et al., 2022*). Southwest of our *P. pepei* site, in  
509 the central Andes of southern Peru ice proxy data indicated recent surface warming in the tropics that appears unprecedented  
510 in 5000 years (*Thompson et al., 2006*). In November 2009 near Keara, temperatures were so warm that a catastrophic glacial  
511 lake outburst flood eliminated roads, livestock, and structures in the small community (< 3800 m.a.s.l.; *Hoffmann and*  
512 *Weggenmann, 2013*).

513

514 Several observational climate studies have reported a delay in the onset of the wet season in the tropical Andes and southern  
515 Amazon Basin (> ~15°S), especially since the 1990s (*Espinoza et al., 2016; Fu et al., 2013; Marengo et al., 2011*). One possible  
516 explanation is that an intensification of the atmospheric Hadley circulation, related to warming in the (northern) tropical  
517 Atlantic Ocean, has led to an interruption of upward flow from the Amazon during the dry-to-wet period (*Beveridge et al.,*  
518 *2024; Espinoza et al., 2021, 2019; Yoon and Zeng, 2010*). In particular, *Ronchail et al. (2018)* and *Espinoza et al. (2019)* found  
519 a significant increase in dry-day frequency between September-November (austral spring) which marks a delay in the timing  
520 of the wet season in Peru and Bolivia since the late 1990s. All these studies, which are based on *in situ* station and gridded  
521 climate records, argue that warming of the Atlantic, land-surface changes in the Amazon, and wind anomalies are the primary  
522 factors contributing to decreased specific humidity in the central tropical Andes. However, these mechanisms are complex,  
523 and their impacts are spatially variable.

524

525 Overall, the recent negative trend of *P. pepei* RW studied here may be related to temperature-driven moisture trends observed  
526 on both local and regional scales. This study herein has demonstrated the dendroclimatic potential of this species at a treeline  
527 from the most biodiverse region of the world (*Muller, 2017*) and provided insight into the growth response of a tropical forest  
528 in South America to climatic change. High mountain paleoclimate proxies, like our *P. pepei* site, independently show how  
529 temperature-driven humidity changes modify natural environments in tropical South America.



530

## 531 **5. Conclusions**

532 We reported a significant decline in radial growth in a tropical treeline in Bolivia composed by *P. pepei*, in contrast to growth  
533 increases that have been observed in mid-elevation species from the same area of MNP (e.g. *Juglans boliviana*, Oelkers et al.  
534 2023). Several studies have reported on the observed increased dry season length in the southern Amazon and central tropical  
535 Andes, while lowland areas such as the northern Amazon and Andes-Amazon basin (< 2000 m.a.s.l.) are becoming wetter in  
536 the wet-dry season (Arias et al., 2021; Espinoza et al., 2021, 2019; Malhi et al., 2008; Zanin and Satyamurty, 2020). Our results  
537 show that the observed decline in *P. pepei* treeline may be associated with increases in minimum temperatures driven a  
538 reduction of available moisture through different mechanisms resulting in drought stress. Climate-growth correlations showed  
539 *P. pepei* RW was smaller if the prior-year wet season was warmer and drier at the Keara treeline. By expanding the *P. pepei*  
540 network in Keara and the tropical Andes, there is the potential for reconstructions of precipitation and temperature, and thus  
541 drought, for the Central Andes. This would be the first of its kind for northern Bolivia, extending the limited station records  
542 (~30 years in length on average) back to at least the 1800s. The results presented herein have provided insights into the response  
543 of a tropical Andean treeline in an era of global warming, increasing climate extremes, and human activities, and support the  
544 use of dendrochronology in future research of tropical forests.

545

## 546 **Code and Data Availability**

547 R and python codes will be deposited on a Zenodo Archive. The final RW chronology from Keara will be made available on  
548 the NOAA International Tree-ring Database.

549

## 550 **Author contribution**

551 Co-authors LAH, DRC, MRC, MEF, RO, ET collected tree samples in Keara. Tree-ring dating, measuring, and analyses was  
552 conducted by corresponding other RO. Site images for figure 1 were taken by RO.

## 553 **Competing interests**

554 The authors declare that they have no conflict of interest

555



## 556 Acknowledgements

557 This work was made possible by the following funding sources from the U.S. National Science Foundation: AGS-1702789,  
558 AGS-1903687, AGS-2303524, and OISE-1743738. We acknowledge the NSF AGS-1903690 grant at UC Irvine KCCAMS  
559 facility for seven radiocarbon measurements. E.T. received funding from the Comunidad de Madrid program Atracción  
560 Talento “César Nombela” grant number 2023-T1/ECO-29118. We would also like to thank Renaud, his family and the  
561 community of Keara for their hospitality, knowledge, and assistance in the field. Special thanks to Freddy “Zen” Ruiz from  
562 the Nacional Herbario in La Paz for his guidance during the 2019 Bolivian field campaigns.

563

564

## 565 References

- 566 Akaike, H., 1974. A new look at the statistical model identification. *IEEE Trans. Autom. Control* 19, 716–723.
- 567 Álvarez, C., Veblen, T.T., Christie, D.A., González-Reyes, Á., 2015. Relationships between climate variability and radial  
568 growth of *Nothofagus pumilio* near altitudinal treeline in the Andes of northern Patagonia, Chile. *For. Ecol. Manag.*  
569 342, 112–121. <https://doi.org/10.1016/j.foreco.2015.01.018>
- 570 Andreu-Hayles, L., Tejedor, E., D’Arrigo, R., Locosselli, G.M., Rodríguez-Catón, M., Daux, V., Oelkers, R., Pacheco-Solana,  
571 A., Paredes-Villanueva, K., Rodríguez-Morata, C., 2023. Dendrochronological advances in the tropical and  
572 subtropical Americas: Research priorities and future directions. *Dendrochronologia* 81, 126124.  
573 <https://doi.org/10.1016/j.dendro.2023.126124>
- 574 Arias, P.A., Garreaud, R., Poveda, G., Espinoza, J.C., Molina-Carpio, J., Masiokas, M., Viale, M., Scaff, L., van Oevelen, P.J.,  
575 2021. Hydroclimate of the Andes Part II: Hydroclimate Variability and Sub-Continental Patterns. *Front. Earth Sci.* 8.  
576 <https://doi.org/10.3389/feart.2020.505467>
- 577 Batllori, E., Gutiérrez, E., 2008. Regional tree line dynamics in response to global change in the Pyrenees. *J. Ecol.* 96, 1275–  
578 1288. <https://doi.org/10.1111/j.1365-2745.2008.01429.x>
- 579 Beveridge, C.F., Espinoza, J.-C., Athayde, S., Correa, S.B., Couto, T.B.A., Heilpern, S.A., Jenkins, C.N., Piland, N.C.,  
580 Utsunomiya, R., Wongchuig, S., Anderson, E.P., 2024. The Andes–Amazon–Atlantic pathway: A foundational  
581 hydroclimate system for social–ecological system sustainability. *Proc. Natl. Acad. Sci.* 121, e2306229121.  
582 <https://doi.org/10.1073/pnas.2306229121>
- 583 Buras, A., 2017. A comment on the expressed population signal. *Dendrochronologia* 44, 130–132.  
584 <https://doi.org/10.1016/j.dendro.2017.03.005>
- 585 Camarero, J.J., Menvielso, H.A., Sánchez-Salguero, R., 2020. How Past and Future Climate and Drought Drive Radial-  
586 Growth Variability of Three Tree Species in a Bolivian Tropical Dry Forest, in: Pompa-García, M., Camarero, J.J.  
587 (Eds.), *Latin American Dendroecology: Combining Tree-Ring Sciences and Ecology in a Megadiverse Territory*.  
588 Springer International Publishing, Cham, pp. 141–167. [https://doi.org/10.1007/978-3-030-36930-9\\_7](https://doi.org/10.1007/978-3-030-36930-9_7)
- 589 Chavez, S.P., Takahashi, K., 2017. Orographic rainfall hot spots in the Andes–Amazon transition according to the TRMM  
590 precipitation radar and in situ data. *J. Geophys. Res. Atmospheres* 122, 5870–5882.  
591 <https://doi.org/10.1002/2016JD026282>
- 592 Cook, E.R., Briffa, K.R., Shiyatov, S., Mazepa, V., 1990. Tree-ring standardization and growth-trend estimation 104–123.
- 593 Cook, E.R., Peters, K., 1981. The Smoothing Spline: A New Approach to Standardizing Forest Interior Tree-Ring Width Series  
594 for Dendroclimatic Studies.
- 595 Cuesta, F., Tovar, C., Llambí, L.D., Gosling, W.D., Halloy, S., Carilla, J., Muriel, P., Meneses, R.I., Beck, S., Ulloa Ulloa, C.,  
596 Yager, K., Aguirre, N., Viñas, P., Jácome, J., Suárez-Duque, D., Buytaert, W., Pauli, H., 2020. Thermal niche traits



- 597 of high alpine plant species and communities across the tropical Andes and their vulnerability to global warming. *J.*  
598 *Biogeogr.* 47, 408–420. <https://doi.org/10.1111/jbi.13759>
- 599 Cuyckens, G.A.E., Christie, D.A., Domic, A.I., Malizia, L.R., Renison, D., 2016. Climate change and the distribution and  
600 conservation of the world’s highest elevation woodlands in the South American Altiplano. *Glob. Planet. Change* 137,  
601 79–87. <https://doi.org/10.1016/j.gloplacha.2015.12.010>
- 602 Cybis Elektronik, 2010. CDendro and CooRecorder [WWW Document]. URL <http://www.cybis.se/forfun/dendro/index.htm>
- 603 D’Arrigo, R., Wilson, R., Liepert, B., Cherubini, P., 2008. On the ‘Divergence Problem’ in Northern Forests: A review of the  
604 tree-ring evidence and possible causes. *Glob. Planet. Change* 60, 289–305.  
605 <https://doi.org/10.1016/j.gloplacha.2007.03.004>
- 606 D’Arrigo, R.D., Kaufmann, R.K., Davi, N., Jacoby, G.C., Laskowski, C., Myneni, R.B., Cherubini, P., 2004. Thresholds for  
607 warming-induced growth decline at elevational tree line in the Yukon Territory, Canada. *Glob. Biogeochem. Cycles*  
608 18. <https://doi.org/10.1029/2004GB002249>
- 609 Devi, N.M., Kukarskih, V.V., Galimova, A.A., Mazepa, V.S., Grigoriev, A.A., 2020. Climate change evidence in tree growth  
610 and stand productivity at the upper treeline ecotone in the Polar Ural Mountains. *For. Ecosyst.* 7, 7.  
611 <https://doi.org/10.1186/s40663-020-0216-9>
- 612 Duque, A., Peña, M.A., Cuesta, F., González-Caro, S., Kennedy, P., Phillips, O.L., Calderón-Loor, M., Blundo, C., Carilla, J.,  
613 Cayola, L., Farfán-Ríos, W., Fuentes, A., Grau, R., Homeier, J., Loza-Rivera, M.I., Malhi, Y., Malizia, A., Malizia,  
614 L., Martínez-Villa, J.A., Myers, J.A., Osinaga-Acosta, O., Peralvo, M., Pinto, E., Saatchi, S., Silman, M., Tello, J.S.,  
615 Terán-Valdez, A., Feeley, K.J., 2021. Mature Andean forests as globally important carbon sinks and future carbon  
616 refuges. *Nat. Commun.* 12, 2138. <https://doi.org/10.1038/s41467-021-22459-8>
- 617 Enfield, D.B., Mestas-Nuñez, A.M., Mayer, D.A., Cid-Serrano, L., 1999. How ubiquitous is the dipole relationship in tropical  
618 Atlantic sea surface temperatures? *J. Geophys. Res. Oceans* 104, 7841–7848. <https://doi.org/10.1029/1998JC900109>
- 619 Espinoza, J.-C., Arias, P.A., Moron, V., Junquas, C., Segura, H., Sierra-Pérez, J.P., Wongchuig, S., Condom, T., 2021. Recent  
620 Changes in the Atmospheric Circulation Patterns during the Dry-to-Wet Transition Season in South Tropical South  
621 America (1979–2020): Impacts on Precipitation and Fire Season. *J. Clim.* 34, 9025–9042.  
622 <https://doi.org/10.1175/JCLI-D-21-0303.1>
- 623 Espinoza, J.C., Ronchail, J., Marengo, J.A., Segura, H., 2019. Contrasting North–South changes in Amazon wet-day and dry-  
624 day frequency and related atmospheric features (1981–2017). *Clim. Dyn.* 52, 5413–5430.  
625 <https://doi.org/10.1007/s00382-018-4462-2>
- 626 Espinoza, J.C., Segura, H., Ronchail, J., Drapeau, G., Gutierrez-Cori, O., 2016. Evolution of wet-day and dry-day frequency  
627 in the western Amazon basin: Relationship with atmospheric circulation and impacts on vegetation. *Water Resour.*  
628 *Res.* 52, 8546–8560. <https://doi.org/10.1002/2016WR019305>
- 629 Espinoza, T.E.B., Kessler, M., 2022. A monograph of the genus *Polylepis* (Rosaceae). *PhytoKeys* 203, 1–274.  
630 <https://doi.org/10.3897/phytokeys.203.83529>
- 631 Feeley, K.J., Rehm, E.M., Machovina, B., 2012. perspective: The responses of tropical forest species to global climate change:  
632 acclimate, adapt, migrate, or go extinct? *Front. Biogeogr.* 4. <https://doi.org/10.21425/F5FBG12621>
- 633 Feeley, K.J., Silman, M.R., Bush, M.B., Farfan, W., Cabrera, K.G., Malhi, Y., Meir, P., Revilla, N.S., Quisíyupanqui, M.N.R.,  
634 Saatchi, S., 2011. Upslope migration of Andean trees. *J. Biogeogr.* 38, 783–791. <https://doi.org/10.1111/j.1365-2699.2010.02444.x>
- 635 Ferrero, M.E., Villalba, R., De Membiela, M., Ripalta, A., Delgado, S., Paolini, L., 2013. Tree-growth responses across  
636 environmental gradients in subtropical Argentinean forests. *Plant Ecol.* 214, 1321–1334.  
637 <https://doi.org/10.1007/s11258-013-0254-2>
- 638 Finer, M., Mamani, N., 2023. Amazon Deforestation & Fire Hotspots 2022. *MAAP* 187, 2017–21.
- 640 Flynn, H., Camarero, J.J., Sanmiguel-Valladolid, A., Rojas Heredia, F., Domínguez Aguilar, P., Revuelto, J., López-Moreno,  
641 J.I., 2025. A shift in circadian stem increment patterns in a Pyrenean alpine treeline precedes spring growth after snow  
642 melting. *Biogeosciences* 22, 1135–1147. <https://doi.org/10.5194/bg-22-1135-2025>
- 643 Frank, D., Esper, J., Cook, E., 2006. On variance adjustments in tree-ring chronology development. *Tree Rings Archaeol.*  
644 *Climatol. Ecol. TRACE* 4, 56–66.
- 645 Fritts, H.C., 1976. *Tree rings and Climate*. Academic Press, London.



- 646 Fu, R., Yin, L., Li, W., Arias, P.A., Dickinson, R.E., Huang, L., Chakraborty, S., Fernandes, K., Liebmann, B., Fisher, R.,  
647 Myneni, R.B., 2013. Increased dry-season length over southern Amazonia in recent decades and its implication for  
648 future climate projection. *Proc. Natl. Acad. Sci.* 110, 18110–18115. <https://doi.org/10.1073/pnas.1302584110>
- 649 Fuentes, A., 2005. Una introducción a la vegetación de la región de Madidi 32.
- 650 Funk, C., Peterson, P., Landsfeld, M., Pedreros, D., Verdin, J., Shukla, S., Husak, G., Rowland, J., Harrison, L., Hoell, A.,  
651 2015. The climate hazards infrared precipitation with stations—a new environmental record for monitoring extremes.  
652 *Sci. Data* 2, 1–21.
- 653 García-Núñez, C., Rada, F., Boero, C., González, J., Gallardo, M., Azócar, A., Liberman-Cruz, M., Hilal, M., Prado, F., 2004.  
654 Leaf Gas Exchange and Water Relations in *Polylepis tarapacana* at Extreme Altitudes in the Bolivian Andes.  
655 *Photosynthetica* 42, 133–138. <https://doi.org/10.1023/B:PHOT.0000040581.94641.ed>
- 656 Garreaud, R., 1999. Multiscale Analysis of the Summertime Precipitation over the Central Andes.
- 657 Garreaud, R.D., 2009. The Andes climate and weather. *Adv. Geosci.* 22, 3–11. <https://doi.org/10.5194/adgeo-22-3-2009>
- 658 Good, P., Lowe, J.A., Collins, M., Moufouma-Okia, W., 2008. An objective tropical Atlantic sea surface temperature gradient  
659 index for studies of south Amazon dry-season climate variability and change. *Philos. Trans. R. Soc. B Biol. Sci.* 363,  
660 1761–1766. <https://doi.org/10.1098/rstb.2007.0024>
- 661 Groenendijk, P., Babst, F., Trouet, V., Fan, Z.-X., Granato-Souza, D., Locosselli, G.M., Mokria, M., Panthi, S., Pumijunnong,  
662 N., Abiyu, A., Acuña-Soto, R., Adeniesky-Filho, E., Alfaro-Sánchez, R., Anholetto Junior, C.R., Aragão, J.R.V.,  
663 Assis-Pereira, G., Astudillo-Sánchez, C.C., Carolina Barbosa, A., Barreto, N. de O., Battipaglia, G., Beeckman, H.,  
664 Botosso, P.C., Bourland, N., Bräuning, A., Brienen, R., Brookhouse, M., Buajan, S., Buckley, B.M., Camarero, J.J.,  
665 Carrillo-Parra, A., Ceccantini, G., Centeno-Erguera, L.R., Cerano-Paredes, J., Cervantes-Martínez, R., Chanthorn,  
666 W., Chen, Y.-J., Cintra, B.B.L., Cornejo-Oviedo, E.H., Cortés-Cortés, O., Costa, C.M., Couralet, C., Crispin-  
667 Delacruz, D.B., D’Arrigo, R., David, D.A., De Ridder, M., Del Valle, J.I., Díaz-Carrillo, O.A., Dobner Jr, M., Doucet,  
668 J.-L., Dünisch, O., Enquist, B.J., Esemann-Quadros, K., Esquivel-Arriaga, G., Fayolle, A., Fenilli, T.A.B., Ferrero,  
669 M.E., Fichtler, E., Finnegan, P.M., Fontana, C., Francisco, K.S., Fu, P.-L., Galvão, F., Gebrekirstos, A., Giraldo, J.A.,  
670 Gloor, E., Godoy-Veiga, M., Guerra, A., Haneca, K., Harley, G.L., Heinrich, I., Helle, G., Hernández-Díaz, J.C.,  
671 Hornink, B., Hubau, W., Inga, J.G., Islam, M., Jiang, Y., Kaib, M., Hassan Khamisi, Z., Koprowski, M., Layme, E.,  
672 Leffler, A.J., Ligot, G., Lisi, C.S., Loader, N.J., Lobo, F. de A., Longhi-Santos, T., Lopez, L., López-Hernández, M.I.,  
673 Lousada, J.L.P.C., Manzanedo, R.D., Marcon, A.K., Maxwell, J.T., Mendivelso, H.A., Mendoza-Villa, O.N.,  
674 Menezes, Í.R.N., Montóia, V.R., Moors, E., Moreno, M., Muñoz-Castro, M.A., Nabais, C., Nathalang, A., Ngoma, J.,  
675 Nogueira Jr., F. de C., Oliveira, J.M., Olmedo, G.M., Ortega-Rodriguez, D.R., Ortiz, C.E.R., Pagotto, M.A., Paredes-  
676 Villanueva, K., Pérez-De-Lis, G., Ponce Calderón, L.P., Portal-Cahuana, L.A., Pucha-Cofrep, D.A., Quadri, P.,  
677 Rahman, M., Ramírez, J.A., Requena-Rojas, E.J., Reyes-Flores, J., Ribeiro, A. de S., Robertson, I., Roig, F.A.,  
678 Roquette, J.G., Rubio-Camacho, E.A., Sánchez-Salguero, R., Sass-Klaassen, U., Schöngart, J., Scipioni, M.C.,  
679 Sheppard, P.R., Silva, L.C.R., Slotta, F., Soria-Díaz, L., Sousa, L.K.V.S., Speer, J.H., Therrell, M.D., Ticse-Otarola,  
680 G., Tomazello-Filho, M., Torbenson, M.C.A., Tor-Ngern, P., Touchan, R., Van Den Bulcke, J., Vázquez-Selem, L.,  
681 Velázquez-Pérez, A.H., Venegas-González, A., Villalba, R., Villanueva-Díaz, J., Vlam, M., Vourlitis, G., Wehenkel,  
682 C., Wils, T., Zavaleta, E.S., Zewdu, E.A., Zhang, Y.-J., Zhou, Z.-K., Zuidema, P.A., 2025. The importance of tropical  
683 tree-ring chronologies for global change research. *Quat. Sci. Rev.* 355, 109233.  
684 <https://doi.org/10.1016/j.quascirev.2025.109233>
- 685 Harris, I., Osborn, T.J., Jones, P., Lister, D., 2020. Version 4 of the CRU TS monthly high-resolution gridded multivariate  
686 climate dataset. *Sci. Data* 7, 109. <https://doi.org/10.1038/s41597-020-0453-3>
- 687 Haurwitz, M.W., Brier, G.W., 1981. A critique of the superposed epoch analysis method: its application to solar–weather  
688 relations. *Mon. Weather Rev.* 109, 2074–2079.
- 689 Hertel, D., Wesche, K., 2008. Tropical moist *Polylepis* stands at the treeline in East Bolivia: the effect of elevation on stand  
690 microclimate, above- and below-ground structure, and regeneration. *Trees* 22, 303–315.  
691 <https://doi.org/10.1007/s00468-007-0185-4>
- 692 Hoch, G., Körner, C., 2005. Growth, Demography and Carbon Relations of *Polylepis* Trees at the World’s Highest Treeline.  
693 *Funct. Ecol.* 19, 941–951.
- 694 Hock, R., Rasul, G., Adler, C., Caceres, B., Gruber, S., Hirabayashi, Y., Jackson, M., Käab, A., Kang, S., Kutuzov, S., Milner,  
695 A., Molau, U., Morin, S., Orlove, B., Steltzer, H., Allen, S., Arenson, L., Banerjee, S., Barr, I., Bórquez, R., Brown,



- 696 L., Cao, B., Carey, M., Cogley, G., Fischlin, A., A de Sherbinin, Eckert, N., Geertsema, M., Hagenstad, M., Honsberg,  
697 M., Hood, E., Huss, M., E Jimenez Zamora, Kotlarski, S., Lefeuvre, P., J Ignacio López Moreno, Lundquist, J.,  
698 Mcdowell, G., Mills, S., Mou, C., Nepal, S., Noetzli, J., Palazzi, E., Pepin, N., Rixen, C., Shahgedanova, M., S  
699 McKenzie Skiles, Vincent, C., Viviroli, D., Gesa, A.W., P Yangjee Sherpa, Weyer, N., Wouters, B., Yasunari, T.,  
700 You, Q., Zhang, Y., 2019. High Mountain Areas. STATI UNITI D'AMERICA.
- 701 Hoffmann, D., Weggenmann, D., 2013. Climate Change Induced Glacier Retreat and Risk Management: Glacial Lake Outburst  
702 Floods (GLOFs) in the Apolobamba Mountain Range, Bolivia, in: Leal Filho, W. (Ed.), Climate Change and Disaster  
703 Risk Management, Climate Change Management. Springer, Berlin, Heidelberg, pp. 71–87.  
704 [https://doi.org/10.1007/978-3-642-31110-9\\_5](https://doi.org/10.1007/978-3-642-31110-9_5)
- 705 Hua, Q., Turnbull, J.C., Santos, G.M., Rakowski, A.Z., Ancapichún, S., Pol-Holz, R.D., Hammer, S., Lehman, S.J., Levin, I.,  
706 Miller, J.B., Palmer, J.G., Turney, C.S.M., 2022. ATMOSPHERIC RADIOCARBON FOR THE PERIOD 1950–  
707 2019. Radiocarbon 64, 723–745. <https://doi.org/10.1017/RDC.2021.95>
- 708 Jacoby, G.C., D'Arrigo, R.D., 1995. Tree ring width and density evidence of climatic and potential forest change in Alaska.  
709 Glob. Biogeochem. Cycles 9, 227–234. <https://doi.org/10.1029/95GB00321>
- 710 Jaramillo, A.D., 2015. Fotosíntesis en los Bosques a Mayor Elevación en el Planeta: *Polylepis tarapacana* en un Gradiente de  
711 Elevación en los Andes de Arica y Parinacota, Chile.
- 712 Jomelli, V., Pavlova, I., Guin, O., Soliz-Gamboa, C., Contreras, A., Toivonen, J.M., Zetterberg, P., 2012. Analysis of the  
713 Dendroclimatic Potential of *Polylepis pepei*, *P. subsericans* and *P. rugulosa* In the Tropical Andes (Peru-Bolivia).  
714 Tree-Ring Res. 68, 91–103. <https://doi.org/10.3959/2011-10.1>
- 715 Junquas, C., Takahashi, K., Condom, T., Espinoza, J.-C., Chavez, S., Sicart, J.-E., Lebel, T., 2018. Understanding the influence  
716 of orography on the precipitation diurnal cycle and the associated atmospheric processes in the central Andes. Clim.  
717 Dyn. 50, 3995–4017. <https://doi.org/10.1007/s00382-017-3858-8>
- 718 Kessler, M., Toivonen, J.M., Sylvester, S.P., Kluge, J., Hertel, D., 2014. Elevational patterns of *Polylepis* tree height  
719 (*Rosaceae*) in the high Andes of Peru: role of human impact and climatic conditions. Front. Plant Sci. 5.  
720 <https://doi.org/10.3389/fpls.2014.00194>
- 721 Kolmogorov, A., 1933. Sulla determinazione empirica di una legge di distribuzione. Giorn Dellinst Ital Degli Att 4, 89–91.
- 722 Körner, C., 2012. Definitions and conventions, in: Körner, C. (Ed.), Alpine Treelines: Functional Ecology of the Global High  
723 Elevation Tree Limits. Springer, Basel, pp. 11–19. [https://doi.org/10.1007/978-3-0348-0396-0\\_2](https://doi.org/10.1007/978-3-0348-0396-0_2)
- 724 Körner, C., Hoch, G., 2023. Not every high-latitude or high-elevation forest edge is a treeline. J. Biogeogr. 50, 838–845.  
725 <https://doi.org/10.1111/jbi.14593>
- 726 Locosselli, G.M., Brien, R.J.W., Leite, M. de S., Gloor, M., Krottenthaler, S., Oliveira, A.A. de, Barichivich, J., Anhof, D.,  
727 Ceccantini, G., Schöngart, J., Buckeridge, M., 2020. Global tree-ring analysis reveals rapid decrease in tropical tree  
728 longevity with temperature. Proc. Natl. Acad. Sci. 117, 33358–33364. <https://doi.org/10.1073/pnas.2003873117>
- 729 López, V.L., Huertas Herrera, A., Rosas, Y.M., Cellini, J.M., 2022. Optimal environmental drivers of high-mountains forest:  
730 *Polylepis tarapacana* cover evaluation in their southernmost distribution range of the Andes. Trees For. People 9,  
731 100321. <https://doi.org/10.1016/j.tfp.2022.100321>
- 732 Macek, P., Macková, J., de Bello, F., 2009. Morphological and ecophysiological traits shaping altitudinal distribution of three  
733 *Polylepis* treeline species in the dry tropical Andes. Acta Oecologica 35, 778–785.  
734 <https://doi.org/10.1016/j.actao.2009.08.013>
- 735 Macía, M.J., 2008. Woody plants diversity, floristic composition and land use history in the Amazonian rain forests of Madidi  
736 National Park, Bolivia. Biodivers. Conserv. 17, 2671–2690. <https://doi.org/10.1007/s10531-008-9348-x>
- 737 Malhi, Y., Roberts, J.T., Betts, R.A., Killeen, T.J., Li, W., Nobre, C.A., 2008. Climate Change, Deforestation, and the Fate of  
738 the Amazon. Science 319, 169–172.
- 739 Malizia, A., Blundo, C., Carilla, J., Acosta, O.O., Cuesta, F., Duque, A., Aguirre, N., Aguirre, Z., Ataroff, M., Baez, S.,  
740 Calderón-Loor, M., Cayola, L., Cayuela, L., Ceballos, S., Cedillo, H., Rios, W.F., Feeley, K.J., Fuentes, A.F., Álvarez,  
741 L.E.G., Grau, R., Homeier, J., Jadan, O., Llambi, L.D., Rivera, M.I.L., Macía, M.J., Malhi, Y., Malizia, L., Peralvo,  
742 M., Pinto, E., Tello, S., Silman, M., Young, K.R., 2020. Elevation and latitude drives structure and tree species  
743 composition in Andean forests: Results from a large-scale plot network. PLOS ONE 15, e0231553.  
744 <https://doi.org/10.1371/journal.pone.0231553>



- 745 Marengo, J.A., Tomasella, J., Alves, L.M., Soares, W.R., Rodriguez, D.A., 2011. The drought of 2010 in the context of  
746 historical droughts in the Amazon region. *Geophys. Res. Lett.* 38. <https://doi.org/10.1029/2011GL047436>
- 747 Meko, D.M., Touchan, R., Anchukaitis, K.J., 2011. Seascorr: A MATLAB program for identifying the seasonal climate signal  
748 in an annual tree-ring time series. *Comput. Geosci.* 37, 1234–1241. <https://doi.org/10.1016/j.cageo.2011.01.013>
- 749 Melvin, T., 2004. Historical growth rates and changing climatic sensitivity of boreal conifers.
- 750 Montaña-Centellas, F., Fuentes, A.F., Cayola, L., Macía, M.J., Arellano, G., Loza, M.I., Nieto-Ariza, B., Tello, J.S., 2024.  
751 Elevational range sizes of woody plants increase with climate variability in the Tropical Andes. *J. Biogeogr.* 51, 814–  
752 826. <https://doi.org/10.1111/jbi.14783>
- 753 Morales, M.S., Crispín-DelaCruz, D.B., Álvarez, C., Christie, D.A., Ferrero, M.E., Andreu-Hayles, L., Villalba, R., Guerra,  
754 A., Ticse-Otarola, G., Rodríguez-Ramírez, E.C., LLocella-Martínez, R., Sanchez-Ferrer, J., Requena-Rojas, E.J.,  
755 2023. Drought increase since the mid-20th century in the northern South American Altiplano revealed by a 389-year  
756 precipitation record. *Clim. Past* 19, 457–476. <https://doi.org/10.5194/cp-19-457-2023>
- 757 Morales, M.S., Villalba, R., Grau, H.R., Paolini, L., 2004. Rainfall-Controlled Tree Growth in High-Elevation Subtropical  
758 Treelines. *Ecology* 85, 3080–3089. <https://doi.org/10.1890/04-0139>
- 759 Muller, M.R., 2017. Protected areas and their relationship with food security in a context of climate change: an overview from  
760 Bolivia, Brazil and Peru. *Prot. AREAS.*
- 761 Navarro, G., Arrázola, S., Balderrama, J.A., Ferreira, W., De la Barra, N., Antezana, C., Gómez, I., Mercado, M., 2010.  
762 Diagnóstico del estado de conservación y caracterización de los bosques de *Polylepis* en Bolivia y su avifauna  
763 Conservation state analysis and characterization of the Bolivian *Polylepis* forests and their avifauna. *Rev. Boliv. Ecol.*  
764 *Conserv. Ambient.* 28, 1–35.
- 765 Oelkers, R.C., Andreu-Hayles, L., D'Arrigo, R., Pacheco-Solana, A., Rodriguez-Caton, M., Fuentes, A., Santos, G.M.,  
766 Tejedor, E., Ferrero, M.E., Maldonado, C., 2023. Recent growth increase in endemic *Juglans boliviana* from the  
767 tropical Andes. *Dendrochronologia* 79, 126090. <https://doi.org/10.1016/j.dendro.2023.126090>
- 768 Paegle, J.N., Mo, K.C., 2002. Linkages between Summer Rainfall Variability over South America and Sea Surface  
769 Temperature Anomalies.
- 770 Paulsen, J., Weber, U. M., and Körner, Ch., 2000. Tree Growth near Treeline: Abrupt or Gradual Reduction with Altitude?  
771 *Arct. Antarct. Alp. Res.* 32, 14–20. <https://doi.org/10.1080/15230430.2000.12003334>
- 772 Pettitt, A.N., 1979. A Non-Parametric Approach to the Change-Point Problem. *J. R. Stat. Soc. Ser. C Appl. Stat.* 28, 126–135.  
773 <https://doi.org/10.2307/2346729>
- 774 Quesada-Román, A., Ballesteros-Cánovas, J.A., St. George, S., Stoffel, M., 2022. Tropical and subtropical dendrochronology:  
775 Approaches, applications, and prospects. *Ecol. Indic.* 144, 109506. <https://doi.org/10.1016/j.ecolind.2022.109506>
- 776 Rao, M.P., Cook, E.R., Cook, B.I., Anchukaitis, K.J., D'Arrigo, R.D., Krusic, P.J., LeGrande, A.N., 2019. A double bootstrap  
777 approach to Superposed Epoch Analysis to evaluate response uncertainty. *Dendrochronologia* 55, 119–124.  
778 <https://doi.org/10.1016/j.dendro.2019.05.001>
- 779 Rasmusson, E.M., Carpenter, T.H., 1982. Variations in tropical sea surface temperature and surface wind fields associated  
780 with the Southern Oscillation/El Niño. *Mon. Weather Rev.* 110, 354–384.
- 781 Rehm, E.M., Feeley, K.J., 2013. Forest patches and the upward migration of timberline in the southern Peruvian Andes. *For.*  
782 *Ecol. Manag.* 305, 204–211. <https://doi.org/10.1016/j.foreco.2013.05.041>
- 783 Requena-Rojas, E.J., Amoroso, M.M., Ticse-Otarola, G., Crispín-Delacruz, D.B., 2021. Assessing Dendrochronological  
784 Potential of *Escallonia myrtilloides* in the High Andes of Peru. *Tree-Ring Res.* 77, 41–52.  
785 <https://doi.org/10.3959/TRR2019-8>
- 786 Requena-Rojas, E.J., Crispín-DelaCruz, D.B., Ticse-Otarola, G., Quispe-Melgar, H.R., Inga Guillen, J.G., Camel Paucar, V.,  
787 Guerra, A., Ames-Martínez, F.N., Morales, M., 2020. Temporal Growth Variation in High-Elevation Forests: Case  
788 Study of *Polylepis* Forests in Central Andes, in: Pompa-García, M., Camarero, J.J. (Eds.), *Latin American*  
789 *Dendroecology: Combining Tree-Ring Sciences and Ecology in a Megadiverse Territory.* Springer International  
790 Publishing, Cham, pp. 263–279. [https://doi.org/10.1007/978-3-030-36930-9\\_12](https://doi.org/10.1007/978-3-030-36930-9_12)
- 791 Roig, F., Fernández, M., Gareca León, E., Altamirano, S., Monge, S., 2001. ESTUDIOS DENDROCRONOLÓGICOS EN  
792 LOS AMBIENTES HÚMEDOS DE LA PUNA BOLIVIANA DENDROCHRONOLOGICAL STUDIES IN THE  
793 HUMID PUNA ENVIRONMENTS OF BOLIVIA. *Rev Bol Ecol* 9.



- 794 Rolland, C., Petitcolas, V., Michalet, R., 1998. Changes in radial tree growth for *Picea abies*, *Larix decidua*, *Pinus cembra* and  
795 *Pinus uncinata* near the alpine timberline since 1750. *Trees* 13, 40–53. <https://doi.org/10.1007/PL00009736>
- 796 Romatschke, U., Houze, R.A., 2010. Extreme Summer Convection in South America. <https://doi.org/10.1175/2010JCLI3465.1>
- 797 Ronchail, J., Espinoza, J.C., Drapeau, G., Sabot, M., Cochonneau, G., Schor, T., 2018. The flood recession period in Western  
798 Amazonia and its variability during the 1985–2015 period. *J. Hydrol. Reg. Stud.* 15, 16–30.  
799 <https://doi.org/10.1016/j.ejrh.2017.11.008>
- 800 Ropelewski, C.F., Halpert, M.S., 1987. Global and Regional Scale Precipitation Patterns Associated with the El Niño/Southern  
801 Oscillation.
- 802 Schulman, E., 1956. *Dendroclimatic Changes in Semiarid America*. University of Arizona Press, Tucson, p. 142.
- 803 Segura, H., Espinoza, J.C., Junquas, C., Lebel, T., Vuille, M., Condom, T., 2022. Extreme austral winter precipitation events  
804 over the South-American Altiplano: regional atmospheric features. *Clim. Dyn.* 59, 3069–3086.  
805 <https://doi.org/10.1007/s00382-022-06240-1>
- 806 Sierra, J.P., Junquas, C., Espinoza, J.C., Segura, H., Condom, T., Andrade, M., Molina-Carpio, J., Ticona, L., Mardoñez, V.,  
807 Blacutt, L., Polcher, J., Rabatel, A., Sicart, J.E., 2022. Deforestation impacts on Amazon-Andes hydroclimatic  
808 connectivity. *Clim. Dyn.* 58, 2609–2636. <https://doi.org/10.1007/s00382-021-06025-y>
- 809 Simpson, B.B., 1979. A revision of the genus *Polylepis* (Rosaceae: Sanguisorbeae). *Smithson. Contrib. Bot.*
- 810 Smirnov, N., 1948. Table for estimating the goodness of fit of empirical distributions. *Ann. Math. Stat.* 19, 279–281.
- 811 Srur, A.M., Villalba, R., Rodríguez-Catón, M., Amoroso, M.M., Marcotti, E., 2018. Climate and *Nothofagus pumilio*  
812 Establishment at Upper Treelines in the Patagonian Andes. *Front. Earth Sci.* 6.  
813 <https://doi.org/10.3389/feart.2018.00057>
- 814 Srur, A.M., Villalba, Ricardo, Rodríguez-Catón, Milagros, Amoroso, Mariano M., and Marcotti, E., 2016. Establishment of  
815 *Nothofagus pumilio* at Upper Treelines Across a Precipitation Gradient in the Northern Patagonian Andes. *Arct.*  
816 *Antarct. Alp. Res.* 48, 755–766. <https://doi.org/10.1657/AAAR0016-015>
- 817 Stokes, M.A., Smiley, T.L., 1968. *An introduction to tree-ring dating*. University of Chicago Press, Chicago, Illinois.
- 818 Thompson, L.G., Mosley-Thompson, E., Brecher, H., Davis, M., León, B., Les, D., Lin, P.-N., Mashiotta, T., Mountain, K.,  
819 2006. Abrupt tropical climate change: Past and present. *Proc. Natl. Acad. Sci.* 103, 10536–10543.  
820 <https://doi.org/10.1073/pnas.0603900103>
- 821 Tovar, C., Carril, A.F., Gutiérrez, A.G., Ahrends, A., Fita, L., Zaninelli, P., Flombaum, P., Abarzúa, A.M., Alarcón, D.,  
822 Aschero, V., Báez, S., Barros, A., Carilla, J., Ferrero, M.E., Flantua, S.G.A., Gonzáles, P., Menéndez, C.G., Pérez-  
823 Escobar, O.A., Pauchard, A., Ruscica, R.C., Särkinen, T., Sörensson, A.A., Srur, A., Villalba, R., Hollingsworth,  
824 P.M., 2022. Understanding climate change impacts on biome and plant distributions in the Andes: Challenges and  
825 opportunities. *J. Biogeogr.* 49, 1420–1442. <https://doi.org/10.1111/jbi.14389>
- 826 Vera, C., Higgins, W., Amador, J., Ambrizzi, T., Garreaud, R., Gochis, D., Gutzler, D., Lettenmaier, D., Marengo, J., Mechoso,  
827 C.R., Noguez-Paele, J., Silva Dias, P.L., Zhang, C., 2006. Toward a Unified View of the American Monsoon  
828 Systems. *J. Clim.* 19, 4977–5000. <https://doi.org/10.1175/JCLI3896.1>
- 829 Virtanen, P., Gommers, R., Oliphant, T.E., Haberland, M., Reddy, T., Cournapeau, D., Burovski, E., Peterson, P., Weckesser,  
830 W., Bright, J., 2020. SciPy 1.0: fundamental algorithms for scientific computing in Python. *Nat. Methods* 17, 261–  
831 272.
- 832 von Arx, G., Crivellaro, A., Prendin, A.L., Čufar, K., Carrer, M., 2016. Quantitative Wood Anatomy—Practical Guidelines.  
833 *Front. Plant Sci.* 7.
- 834 Vuille, M., Bradley, R.S., Keimig, F., 2000. Interannual climate variability in the Central Andes and its relation to tropical  
835 Pacific and Atlantic forcing. *J. Geophys. Res. Atmospheres* 105, 12447–12460.  
836 <https://doi.org/10.1029/2000JD900134>
- 837 Waskom, M.L., 2021. seaborn: statistical data visualization. *J. Open Source Softw.* 6, 3021.  
838 <https://doi.org/10.21105/joss.03021>
- 839 Wigley, T.M.L., Briffa, K.R., Jones, P.D., 1984. On the Average Value of Correlated Time Series, with Applications in  
840 Dendroclimatology and Hydrometeorology. *J. Appl. Meteorol. Climatol.* 23, 201–213. [https://doi.org/10.1175/1520-0450\(1984\)023<0201:OTAVOC>2.0.CO;2](https://doi.org/10.1175/1520-0450(1984)023<0201:OTAVOC>2.0.CO;2)
- 842 Wilmsking, M., D'Arrigo, R., Jacoby, G.C., Juday, G.P., 2005. Increased temperature sensitivity and divergent growth trends  
843 in circumpolar boreal forests. *Geophys. Res. Lett.* 32. <https://doi.org/10.1029/2005GL023331>



- 844 Wolter, K., Timlin, M.S., 2011. El Niño/Southern Oscillation behaviour since 1871 as diagnosed in an extended multivariate  
845 ENSO index (MEI.ext). *Int. J. Climatol.* 31, 1074–1087. <https://doi.org/10.1002/joc.2336>
- 846 Yoon, J., Zeng, N., 2010. An Atlantic influence on Amazon rainfall. *Clim. Dyn.* 34, 249–264. [https://doi.org/10.1007/s00382-](https://doi.org/10.1007/s00382-009-0551-6)  
847 009-0551-6
- 848 Young, K.R., León, B., 2006. Tree-line changes along the Andes: implications of spatial patterns and dynamics. *Philos. Trans.*  
849 *R. Soc. B Biol. Sci.* 362, 263–272. <https://doi.org/10.1098/rstb.2006.1986>
- 850 Zang, C., Biondi, F., 2015. treeclim: an R package for the numerical calibration of proxy-climate relationships. *Ecography* 38,  
851 431–436. <https://doi.org/10.1111/ecog.01335>
- 852 Zanin, P.R., Satyamurty, P., 2020. Hydrological processes interconnecting the two largest watersheds of South America from  
853 multi-decadal to inter-annual time scales: A critical review. *Int. J. Climatol.* 40, 4006–4038.  
854 <https://doi.org/10.1002/joc.6442>
- 855 Zapata, F., 2013. A multilocus phylogenetic analysis of *Escallonia* (Escalloniaceae): Diversification in montane South  
856 America. *Am. J. Bot.* 100, 526–545. <https://doi.org/10.3732/ajb.1200297>
- 857